Evaluation of the Distributed Thermal Response Test (DTRT): Nupurinkartano as a case study

Petri Hakala, Annu Martinkauppi, Ilkka Martinkauppi, Nina Leppäharju and Kimmo Korhonen

Petri Hakala, Annu Martinkauppi, Ilkka Martinkauppi, Nina Leppäharju and Kimmo Korhonen

EVALUATION OF THE DISTRIBUTED THERMAL RESPONSE TEST (DTRT): NUPURINKARTANO AS A CASE STUDY

Front cover: GTK's TRT rig ready for DTRT measurement at the study site in Nupurinkartano, Espoo. Photo: Ilkka Martinkauppi, GTK.

The layered thermal conductivity of the bedrock and borehole thermal resistance can be determined with the Distributed Thermal Response Test (DTRT), which is a modification of the conventional Thermal Response Test (TRT). The DTRT enables a more detailed examination of the subsurface thermal properties that are significant in a heterogeneous and anisotropic environment. The objective of this study was to evaluate the DTRT method in its entirety, from measurements to interpretation and the utilization of the results. This report comprises a review of the theory related to the DTRT, a description of the Distributed Temperature Sensing (DTS) method, a case study and comparison of the DTRT method with conventional TRT.

To determine the layered thermal conductivity and borehole thermal resistance, the temperature of the heat carrier fluid was logged with optical fiber cables along the borehole length during different phases of the TRT. Particular interest was paid to borehole recovery after the conventional TRT. The borehole was divided into nine sections, each of 20 meters in length. Then, the infinite line source method combined with the superposition technique (i.e. variable heat rate) was applied to each section, fitting the calculated fluid temperatures to the measured ones and minimizing the error between them. Thus, the layered thermal conductivity and the borehole thermal resistance were assessed.

As a result, the test borehole was considered quite homogeneous, having good thermal conductivity, which nevertheless varied between 2.8–4.2 W/(m·K). The differences in the estimation of the layered thermal conductivity may be attributed to both the measurement technology and interpretation aspects. Because the DTS device was subjected to air temperature variations, the temperature data measured with optical fiber cables was affected by the diurnal air temperature fluctuations. The fact that the temperature strongly affected the heat power leads to the conclusion that the heat power may explain the apparent heterogeneity in thermal conductivity. Moreover, finding the appropriate fitting period and layer sectioning may influence the heterogeneity in thermal conductivity. The borehole geophysical investigations carried out earlier demonstrated that the bedrock is composed of homogeneous granite and is solid, with no significant changes in rock type being detected. The results from the SEM analysis indicated good thermal conductivity because of the reasonably high quartz content. Variations in the estimation of the borehole thermal resistance can be accumulated from the acquired layered thermal conductivity, which was used as an input parameter when optimizing the layered borehole thermal resistance. Besides, the heterogeneity of the borehole thermal resistance could be due to convective heat transfer in the groundwater, which was not considered in this study, or possibly lateral deviation in the U-pipe along the borehole depth.

Keywords (GeoRef Thesaurus, AGI): energy sources, geothermal energy, bedrock, boreholes, temperature logging, thermal conductivity, thermal response test, distributed temperature sensing, Nupurinkartano, Finland

Petri Hakala, Annu Martinkauppi and Ilkka Martinkauppi
Geological Survey of Finland, P.O. Box 97, FI-67101 Kokkola, Finland

E-mail: petri.hakala@gtk.fi

Nina Leppäharju and Kimmo Korhonen
Geological Survey of Finland, P.O. Box 96, FI-02151 Espoo, Finland

Energiakaivoa ympäröivän kallion lämmönjohtavuuden ja kaivon lämpövastuksen vertikaalijakauma on mahdollista selvittää DTRT-menetelmällä (engl. Distributed Thermal Response Test), joka on kehittyneempi versio perinteisestä lämpövastetestistä eli TRT-mittauksesta (engl. Thermal Response Test). DTRT-menetelmä tarjoaa yksityiskohtaisempaa tietoa energiakaivoa ympäröivän kallion termisistä ominaisuuksista, mikä on hyödyllistä erityisesti heterogeenisessa ja anisotrooppisessa ympäristössä. Kun perinteisellä TRT-mittauksella saadaan selvitettyä kyseiset parametrit keskimääräisesti koko kaivosta, DTRT-menetelmä mahdollistaa niiden selvittämisen kerroksittain. Tämän tutkimuksen tarkoituksena on arvioida DTRT-menetelmää kokonaisvaltaisesti mittauksista tulkintaan ja tulkintatulosten hyödynnettävyyteen. Tutkimus sisältää teoriaosuuden DTRT-menetelmään sekä analyyttiseen tulkintamenetelmään liittyen, kuvauksen DTS-menetelmästä (engl. Distributed Temperature Sensing), tapausesimerkin Espoon Nupurinkartanosta sekä DTRT- ja TRT-menetelmien vertailua.

Kallioperän kerroksellisen lämmönjohtavuuden selvittämiseksi lämmönkeruuputkistossa olevan nesteen lämpötilaa mitataan optisilla kuiduilla ennen ja jälkeen TRT-mittauksen. Oleellista on mitata lämpötilaa erityisesti TRT-mittauksen jälkeen, kaivon palautumisvaiheessa. Tässä työssä energiakaivo jaettiin yhdeksään 20 metrin paksuiseen kerrokseen, joihin jokaiseen sovellettiin ääretöntä viivalähdemenetelmää yhdistettynä superpositiotekniikkaan. Näin lämmönjohtavuuden vertikaalijakauma saatiin selvitettyä TRT-mittauksen lämmitys- ja palautumisdatasta, joiden tuloksia myös vertailtiin. Tämän jälkeen ratkaistiin kaivon kerroksellinen lämpövastus TRT-lämmitysdatasta käyttäen em. lämmönjohtavuuden vertikaalijakaumaa.

Loppputuloksena voidaan todeta, että Nupurinkartanon tutkimuskaivoa ympäröivä kallioperä on varsin homogeeninen, vaikka lämmönjohtavuus vaihteleekin 2,8 ja 4,2 W/(m·K):n välillä. Lämmönjohtavuuden vaihteluita voidaan osittain pitää mittaus- ja tulkintateknisistä seikoista aiheutuviksi. DTS-laite, joka oli sijoitettu TRT-vaunun sisälle, altistui lämpötilakäynnille, mikä havaittiin mittaustuloksissa. Koska lämpötila vaikuttaa merkittävästi lämpötehon määrittämiseen ja lämpöteho puolestaan kallion tehollisen lämmönjohtavuuden määrittämiseen, voidaan olettaa tämän tekijän selittävän lämmönjohtavuuden vaihteluita. Eräs vaikuttava tekijä voi olla myös sopivan sovitusvälin valinta. Kohteessa aiemmin tehdyt reikägeofysikaaliset tutkimukset ja SEM-analyysin (engl. Scanning Electronic Microscope) tulokset osoittavat kallioperän olevan homogeenista, varsin kvartsirikasta graniittia, jolla on hyvät lämpöominaisuudet. Vaihtelut kaivon lämpövastuksessa johtunevat ainakin osin siitä, että kerroksittain selvitettyä lämmönjohtavuutta käytettiin lähtötietona optimoitaessa kaivon kerroksellista lämpövastusta. Tällöin mahdollisesti mittauksista, datan laadusta ja tehon määrittelystä aiheutuneet virheet kertautuvat myös kerroksellisen lämpövastuksen määrittelyssä. Toisaalta vaihtelut kaivon lämpövastuksessa voivat aiheutua myös konvektiivisesta lämmönsiirtymisestä pohjavedessä ja keruuputken mahdollisesta lateraalisesta taipumisesta syvyyssuuntaan nähden. Näitä tekijöitä ei tarkasteltu tämän tutkimuksen puitteissa.

Asiasanat (Geosanasto, GTK): energialähteet, geoterminen energia, kallioperä, kairanreiät, lämpötilareikämittaus, lämmönjohtokyky, terminen vastetesti, DTS-menetelmä, Nupurinkartano, Suomi

Petri Hakala, Annu Martinkauppi ja Ilkka Martinkauppi
Geologian tutkimuskeskus, PL 97, 67101 Kokkola

Sähköposti: petri.hakala@gtk.fi

Nina Leppäharju ja Kimmo Korhonen
Geologian tutkimuskeskus, PL 96, 02151 Espoo

-

CONTENTS

SYMBOLS

D	Diameter [m]	T_{in}	Temperature of the heat carrier fluid in down going shank [K]
D_b	Borehole diameter [m]		
D_p	Outer pipe diameter [m]	T_{out}	Temperature of the heat carrier fluid in up going shank [K]
f	Friction factor		
Fo	Dimensionless Fourier number	T_w	Temperature of the borehole wall [K]
$G(r_b,t)$	Dimensionless function		
h	Convective heat transfer coefficient [W/(m² K)]	u_m	Fluid average velocity in the pipe [m s⁻¹]
J_0, J_1, Y_0, Y_1	First and second kind of the Bessel functions	x_c	Shank spacing [m]
		ΔT_{in}	Temperature difference between fluid entering into the borehole and undisturbed ground temperature T_0 [K]
L	Length of the borehole [m]		
Nu	Nusselt number		
p	p-linear correction factor		
Pr	Prandtl number	ΔT_{out}	Temperature difference between fluid coming out from the borehole and undisturbed ground temperature T_0 [K]
q	Heat exchange rate [W/m]		
Q	Power [W]		
Q_{gen}	Heat generation [W/m³]		
r_b	Borehole radius [m]	$\dot{V}$	Volumetric flow rate [m³ s⁻¹]
r_i	Inner radius of the pipe [m]	$\nabla \cdot$	Divergence
r_o	Outer radius of the pipe [m]	∇T	Thermal gradient
Re	Reynolds number	$\rho\, C_p$	Volumetric heat capacity of the pipe [J/m³ K]
R_f	Thermal resistance of the heat carrier fluid [K m W⁻¹]		
		C_p	Heat capacity [J/kg K]
R_g	Thermal resistance of the grout [K m W⁻¹]	α	Thermal diffusivity [m² s⁻¹]
		β_0, β_1	Dimensionless best fit parameters
R_{ig}	Thermal resistance between fluid in inlet pipe and pipe outer radius [K m W⁻¹]	γ	Euler's constant (=0.5772)
		λ	Material thermal conductivity [W m⁻¹ K⁻¹]
R_{og}	Thermal resistance between fluid in outlet pipe and pipe outer radius [K m W⁻¹]	λ_f	Fluid thermal conductivity [W m⁻¹ K⁻¹]
		λ_g	Grout thermal conductivity [W m⁻¹ K⁻¹]
R_p	Thermal resistance through pipe material [K m W⁻¹]	σ	Relation between grout and soil thermal conductivities
R_{tot}	Total thermal resistance [K m W⁻¹]		
T_0	Undisturbed ground temperature [K]	μ	Dynamic viscosity [kg s⁻¹ m⁻¹]
		ρ	Density [kg/m³]
T_f	Average temperature of the heat carrier fluid [K]	v	Fluid kinematic viscosity [m² s⁻¹]

1 INTRODUCTION

Designing a reliable, efficient and lasting borehole heat exchanger (BHE) system requires understanding of the thermophysical properties of the ground surrounding the boreholes. The two most important factors are the thermal conductivity and the temperature of the ground. Both of these notably vary, not only regionally and depending on the rock type, but also very locally, so that although bedrock maps offer useful information at the beginning of the project, *in situ* measurements are needed. Moreover, the properties of the heat exchanger itself affect the efficiency of the system in creating thermal resistance between the heat carrier fluid and the borehole wall. The thermal resistance of the borehole is a complex factor that cannot be reliably calculated, but also needs to be measured.

The conventional and nowadays rather widely used method for evaluating the effective thermal conductivity in the ground and the thermal resistance of a borehole heat exchanger is the Thermal Response Test (TRT). The thermal conductivity measured with the TRT is called the effective thermal conductivity, because it is affected by possible groundwater flow. The idea behind the TRT and the results obtained from the first tests were presented in the early 1980s and mid-1990s (e.g. Mogensen 1983; Eklöf & Gehlin 1996). Since then, there have been no major improvements in the measurement procedure, the equipment or the interpretation methods, as the method is fully applicable and current as such. However, as the method has become increasingly popular and even a required procedure in designing large BHE systems in Europe and globally, the level of equipment, the test providers and knowledge of the method varies. In order to set standards, the International Energy Agency (IEA) launched ECES Annex 21 (Energy Conservation through Energy Storage) to compile TRT experiences worldwide and to provide recommendations on the minimum requirements for the equipment and the interpretation.

Fig. 1. GTK's TRT rig in use. Photo: Ilkka Martinkauppi, GTK.

GTK has been a part of ECES Annex 21 since the beginning in 2007, and the first Thermal Response Test equipment in Finland was built in 2008 (Fig. 1). Since then, GTK has performed around 20 TRTs each year. In early 2012, GTK built another TRT system with some adjustments.

In 2006, Fujii et al. proposed an improved TRT method using optical fiber thermometers, also known as Distributed Temperature Sensing (DTS). With this method, the temperature inside the borehole is logged along its depth after conventional TRT measurement as the borehole is cooling down, i.e. during borehole recovery, thus allowing the effective thermal conductivity of the ground to be determined in layers from the surface to the bottom of the borehole. The method is therefore generally called the Distributed Thermal Response Test (DTRT). The DTRT is merely a modification of the conventional TRT and is based on all the same principles, but it offers a more detailed examination of the subsurface surrounding a borehole. In 2008, Acuña et al. modified the DTRT measurement procedure by placing the optical fiber inside the U-pipe heat exchangers and logging the temperature profile even during the TRT heating phase, thus making it possible to interpret the thermal resistance of the heat exchanger in layers.

With the DTRT, the heterogeneous distribution of ground and BHE thermophysical properties can be revealed. This information can be used in optimizing the BHE system and the depth of the boreholes, and in modeling the temperature development of the borehole field. However, this requires a sophisticated computer model that can take into account the layers from the ground and not simply a homogeneous half-space. So far, the DTRT has not become as popular as the conventional TRT in designing BHE systems, even though the improved method offers some advantages. One of the reasons for this is that DTRT measurements require optical cables and a DTS device, which are expensive and require special expertise. In addition, DTRT interpretation is somewhat more complex and time-consuming than TRT interpretation. The DTRT procedure from measurements to interpretation also takes about three times longer than the conventional TRT procedure.

The objective of this study was to evaluate the DTRT method in its entirety, from measurements to interpretation and the utilization of the results. This report comprises a review of DTRT theory, a description of the DTS method, a case study and comparison of the DTRT method with the conventional TRT.

2 DIFFERENCE BETWEEN CONVENTIONAL AND DISTRIBUTED THERMAL RESPONSE TESTS

The thermal parameters of the bedrock and the borehole together define how the thermal front proceeds in the ground during BHE operation. These parameters, the effective thermal conductivity of the bedrock and the borehole thermal resistance, are evaluated via an experimental *in situ* thermal response test. The method is based on the heat transfer efficiency between the bedrock and the heat carrier fluid that flows inside pipes installed in the borehole. Measured parameters are used as input values when optimizing the required length of BHE systems. The functionality of ground source heat pump (GSHP) systems requires an adequate number and length of the boreholes, but also an optimal spacing between the boreholes to cover the energy requirements. To avoid over- and underdimensioning, it is crucial to evaluate the *in situ* thermal conductivity of the bedrock and the undisturbed ground

temperature, but also the thermal resistance of the borehole. The number of boreholes depends on the available surface area, in addition to the efficiency of heat transfer between the heat carrier fluid and surrounding bedrock. TRTs provide valuable and crucial information on *in situ* thermal parameters of the ground and thus have a major effect on the installation costs and system performance. If the bedrock thermal conductivity is high, heat will be transferred effectively into the bedrock, which directly affects the required length of the BHE. The injection of heat into the bedrock during TRT measurement enables the determination of its effective thermal conductivity, which does not depend on injected heat power if groundwater movements are negligible. However, the lower the thermal resistance is in groundwater-filled boreholes, the larger is the injected heat due to natural convection.

The differences between distributed and conventional thermal response tests are within the interpretation schematic. The usual practice is to only measure fluid temperatures at the inlet and outlet sections of the BHE during TRT measurement while the heat carrier fluid circulates in a closed loop pipe system and is heated up with constant heat power. With this method, we gain knowledge of the effective average borehole parameters that may be affected by groundwater advection. Thermal conductivity and borehole thermal resistance may differ in relation to depth, and the distributed thermal response test is thus necessary to obtain information on the parameter values in each separate layer. This provides that we know the average fluid temperature in these layers, and likewise the heat power injected into the bedrock and the undisturbed initial temperature. If the temperature of the heat carrier fluid is only measured at the ground surface level, the average fluid temperature is then

$$T_f(t) = \frac{T_{in}(t) + T_{out}(t)}{2}, \qquad (1)$$

where T_{in} is the temperature of the heat carrier fluid entering the borehole and T_{out} the temperature in the outlet. The average temperature of the fluid is an essential parameter when evaluating the borehole thermal resistance. If the fluid temperature during the thermal response test is high, heat is poorly transferred into the rock and rock thermal conductivity is less than in the case with a lower average temperature. The better the ground thermal conductivity is, the smaller will be the temperature rise of the heat carrier fluid during the thermal response test, although this also depends on the heat power injected into the borehole. In an ideal situation, pipe shanks in the borehole are separated with spacers and the pipes are close to the borehole wall. This minimizes the thermal coupling between pipe shanks and the temperature difference between heat carrier fluid and borehole wall is small, leading to a low borehole thermal resistance.

There is some evidence that the temperature calculated from the inlet and outlet sections of the BHE overestimates the true average fluid temperature, leading to a larger estimate of the borehole thermal resistance (Marcotte & Pasquier 2008). The arithmetic mean calculated with only two temperature values, the inlet and outlet, is only valid if the supplied heat flux during the TRT is constant along the whole borehole length, which does not strictly occur. Therefore, we introduced a p-linear average method for the mean fluid temperature calculation presented by Marcotte and Pasquier (2008),

$$T_f(t) = T_0 + \frac{p(|\Delta T_{in}|^{p+1} - |\Delta T_{out}|^{p+1})}{(1+p)(|\Delta T_{in}|^{p} - |\Delta T_{out}|^{p})}, \qquad (2)$$

where ΔT_{in} is the temperature difference between fluid entering the borehole and the undisturbed ground temperature T_0, and ΔT_{out} is that between the fluid temperature at the outlet and the undisturbed ground temperature. Figure 2 presents the differences between true average fluid temperature measured down the borehole (solid blue vertical line) and the arithmetic mean measured from the inlet and outlet sections of the BHE (solid black vertical line). The temperature data presented in Figure 2 represent the DTRT measurement recorded at the Nupurinkartano study site. Fluid temperature measurements in the test borehole are presented more detail in Chapter 6. The figure on the left corresponds to the situation at the beginning of heat injection and that on the right at the end of heat injection. As can be seen from Figure 2, the difference between the average temperatures becomes smaller the longer the heat injection has lasted. Marcotte and Pasquier (2008) noted that the best match between the true and p-linear average fluid temperatures occurred when factor p approached the value of -1. Figure 2 also illustrates the average temperature of the heat carrier fluid measured using a p-linear correction factor (solid red vertical line, p → -1), which matches better with the true average temperature than the arithmetic mean measured from the inlet and the outlet of the BHE in the early stage of the heating period.

The distributed thermal response test usually consists of four phases, which are the undisturbed initial state, pre-circulation, heating, and recovery. While the first three of these are compulsory, the recovery period is optional but recommendable. The undisturbed temperature profile of the bedrock must be determined before pre-circulation, heating, or other phases. This profile is crucial when evaluating thermal parameters from the heat injection or recovery data. During the pre-
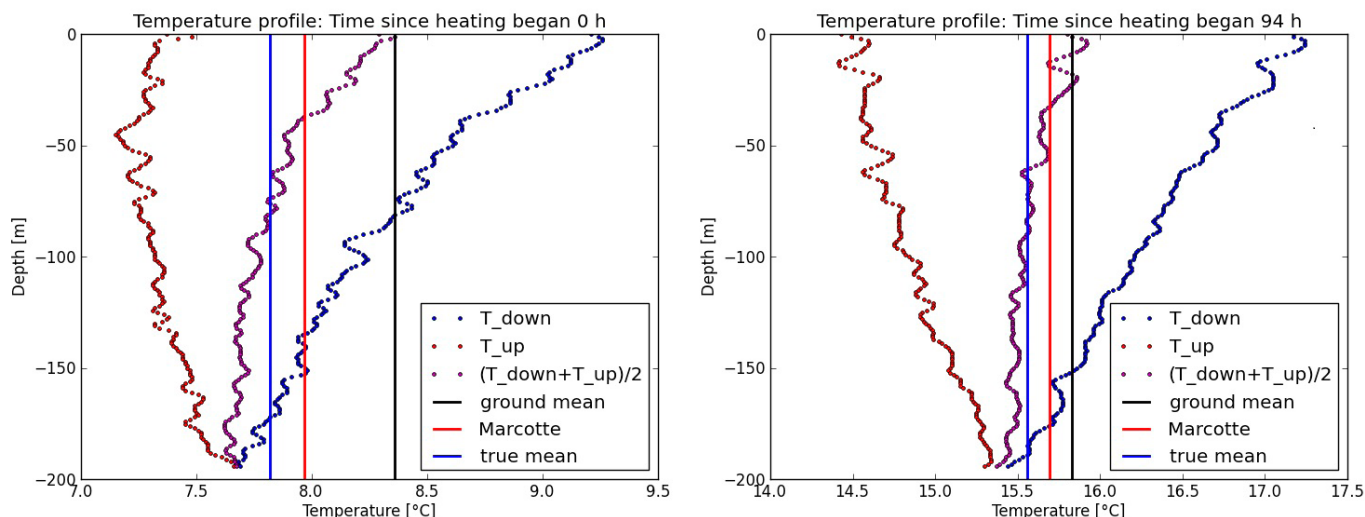
Fig. 2. Fluid temperatures measured at two time points (start and end of heat injection). T_{down} presents the fluid temperature in the descending flow. Photo: Petri Hakala, GTK.

circulation period, fluid circulates in the pipes without heating until the temperature difference between the inlet and the outlet is small enough and the fluid temperature is almost constant along the borehole length. This phase lasts about one hour until the temperature profile is balanced towards the mean of the bedrock in an undisturbed state. When the temperature difference is balanced, electrical resistances in the TRT rig are switched on and fluid is heated up with constant heat power for at least three days. During recovery there is no fluid circulation or heating, and the fluid temperature approaches the undisturbed initial bedrock state.

The conventional thermal response test usually only consists of three phases (undisturbed, pre-circulation, heating), but a recovery period is also helpful if it turns out that the determination of thermal conductivity from the heat injection data is difficult or uncertain. Thermal conductivity can also be obtained from recovery data, which is a good way to validate the result determined from the heating phase. If the recovery period is included in the conventional thermal response test, fluid circulation cannot be stopped after heat injection, which is the case in the distributed thermal response test.

3 ANALYSIS OF HEAT TRANSFER BETWEEN THE BOREHOLE AND THE BEDROCK

The BHE and surrounding bedrock forms a complex system and it is important to understand the theory behind different heat transfer methods. A number of factors affect the efficiency of ground source heat pump systems, including the borehole depth, diameter, and the pipe spacing in the borehole. Material thermal parameters such as thermal conductivity and volumetric heat capacity together define how efficiently heat is transferred from warmer regions to colder ones.

3.1 Thermal resistance of solid and liquid materials

An important parameter when designing BHE systems, in addition to the thermal conductivity of the rock, is the borehole thermal resistance, which defines how effectively heat moves from the borehole wall into the heat carrier fluid, or vice versa. Generally, thermal resistance R is a material property to resist heat transfer between points and surfaces. It is directly proportional to the temperature difference (Monzó 2011):

$$T_2 - T_1 = q \cdot R, \tag{3}$$

where q [W/m] is the heat flow per unit length from the higher temperature point T_2 to the colder one T_1.

The heat transfer efficiency between the heat carrier fluid and the inner pipe surface mainly depends on the pipe dimensions and flow conditions. Heat exchange between the warm heat carrier fluid T_f [K] and colder pipe material T [K] can be calculated using a convective heat flux equation also known as Newton's law of cooling as follows:

$$q'' = h(T_f - T), \tag{4}$$

where the convective heat transfer coefficient h [W/(m²·K)] describes heat transfer due to fluid motion (Incropera & Dewitt 2002). According to equation (3), the thermal resistance [K m W⁻¹] between the fluid and the inner pipe surface is:

$$R_f = \frac{T_f - T}{q} = \frac{T_f - T}{2\pi r_i q''} = \frac{1}{2\pi r_i h}, \tag{5}$$

where r_i is the inner radius of the pipe and T [K] the temperature on the inner pipe surface. The convective heat transfer coefficient h depends on the dimensionless Nusselt number and especially on the pipe geometry (diameter D), and likewise on the fluid velocity profile in the pipes and fluid thermal conductivity λ_f according to the equation

$$h = \frac{\lambda_f}{D} \cdot Nu. \tag{6}$$

If the flow is in a laminar and fully developed state and heat flux on the pipe surface is constant, the Nusselt number is 4.36 (Incropera & Dewitt 2002). Usually, flow is in a turbulent state and the Nusselt number mainly depends on flow velocity and pipe dimensions. In this case, there are several ways to calculate the value for the Nusselt number when turbulent flow conditions are present (Incropera & Dewitt 2002). However, when selecting the proper method, one must be aware of the method limitations. The method introduced in this context is the Gnielinski correlation method, which is

$$Nu = \frac{\left(\frac{f}{8}\right)(Re - 1000)Pr}{1 + 12.7\left(\frac{f}{8}\right)^{0.5}\left(Pr^{\frac{2}{3}} - 1\right)}, \tag{7}$$

where the friction factor f = [0.79 ln(Re) - 1.64]⁻² describes the shear stress between flow and the inner pipe surface. The numeric value of the Nusselt number also depends on the dimensionless Reynolds and Prandtl numbers, Re and Pr. The Gnielinski correlation is only valid if the following criteria are true: 0.5 < Pr < 2000 and 3000 < Re < 5·10⁶. The Reynolds number is an important parameter in fluid mechanics that defines whether the fluid is in laminar or turbulent regime. Its numerical value can be determined from the equation

$$Re = \frac{\rho u_m D}{\mu}, \tag{8}$$

where u_m is the average fluid velocity in the pipes, usually calculated from the known flow rate and pipe cross-section, μ is dynamic viscosity and ρ is fluid density (Incropera & Dewitt 2002). If the Re value is somewhat larger than 2300, flow is in a transition state between laminar and turbulent flow. Flow is fully developed and turbulent when the value is larger than 10 000. Another important parameter in fluid mechanics, in addition to the Reynolds number, is the Prandtl number, which can be calculated as the relationship between the kinematic viscosity ν of a fluid and its thermal diffusivity:

$$Pr = \frac{\nu}{\alpha} = \frac{\mu}{\rho\alpha} = \frac{\mu C_p}{\lambda_f}. \tag{9}$$

Thermal diffusivity α defines how efficiently heat conducts through a material with respect to its volumetric heat capacity ρC_p, i.e.

$$\alpha = \frac{\lambda_f}{\rho C_p}. \tag{10}$$

The convective heat transfer coefficient h is usually quite large, especially if the flow is in the turbulent regime. This means that thermal resistance due to fluid flow is clearly smaller than the resistance between the inner and outer pipe radius. Thermal conduction describes heat flow through a material, and its efficiency depends on the strength of the chemical bonds and internal molecular vibrations. Conduction heat flux through the inner and outer radius of a cylindrical pipe can be calculated from the heat flux equation

$$q'' = -\lambda \frac{dT}{dr}, \tag{11}$$

where λ [W/(m·K)] is the thermal conductivity value of the material (Incropera & Dewitt 2002). For metals like copper, conductivity is clearly larger than that of liquids or gases. Thermal resistance

through pipe material R_p depends on the pipe thermal conductivity and on the inner and outer pipe radius, and it can be calculated according to the equation

$$R_p = \frac{\ln\left(\frac{r_o}{r_i}\right)}{2\pi\lambda_p}. \tag{12}$$

3.2 Theoretical expressions for the thermal resistance of borehole filling material

The thermal resistance for borehole filling material (i.e. grout), R_g, can be estimated using theoretical equations that take into account the thermal conductivity of the material. Some theoretical equations also note the pipe configuration in the borehole. Equations are usually only valid for boreholes grouted with solid material such as Bentonite. Due to natural heat convection in groundwater-filled boreholes, theoretical equations usually overestimate the true thermal resistance, since convection is not taken into account. One must consider groundwater as a solid material in the borehole when calculating its thermal resistance using the equations presented in this chapter.

In the following are presented four different and well-known equations for calculating the thermal resistance of grout. Paul's method (Lamarche et al. 2010) is based on experimental measurements in which the effect of pipe spacing on the thermal resistance of grout was investigated with three different configurations. Measurements showed that thermal resistance is inversely proportional to the product of the grout thermal conductivity and shape factor S_b, i.e.

$$R_g = \frac{1}{S_b\lambda_g} = \frac{1}{\beta_0(r_b/r_o)^{\beta_1}\lambda_g}, \tag{13}$$

where r_o is outer pipe radius and r_b is that of the borehole, and β_0 and β_1 are dimensionless best-fit parameters, whose numeric values are presented in Table 1. The further the pipe shanks are from each other, the lower is the thermal resistance.

Table 1. Beta parameter values for Paul's thermal resistance (Sharqawy et al. 2009).

pipe configuration	β_0	β_1
	20.10	-0.9447
	17.44	-0.6052
	21.91	-0.3796

Another often-used theoretical equation for calculating the thermal resistance of grout is that derived by Hellström (1991), whose equation takes the following form:

$$R_g = \frac{1}{4\pi\lambda_g}\left[\ln\left(\frac{r_b}{r_o}\right) + \ln\left(\frac{r_b}{2x_c}\right) + \right.$$
$$\left. \sigma\ln\left(\frac{(r_b/x_c)^4}{(r_b/x_c)^4 - 1}\right)\right], \tag{14}$$

where the parameter $\sigma = (\lambda_g - \lambda_s)/(\lambda_g + \lambda_s)$ represents the relationship between the thermal conductivities of grout and soil, and x_c is half of the pipe's center-to-center distance, r_b is the borehole radius and r_o the outer radius of the polyethylene pipe. This equation is used in DST software also developed by Hellström (Lamarche et al. 2010).

An improved version of Hellström's equation (14) is that derived by Bennet et al. (1987). The equation is known as the multipole method. Basically, it is the same as Hellström's equation, but it also includes a correction factor, which is the latter parenthesis term in the following equation:

$$R_g = \frac{1}{4\pi\lambda_g}\left[\ln\left(\frac{\lambda_1\lambda_2^{1+4\sigma}}{2(\lambda_2^4 - 1)^\sigma}\right) - \right.$$
$$\left. \left(\frac{\lambda_3^2\left(1 - (4\sigma/(\lambda_2^4 - 1))\right)^2}{1 + \lambda_3^2\left(1 + \left(16\sigma/\left(\lambda_2^2 - \frac{1}{\lambda_2^2}\right)^2\right)\right)}\right)\right], \tag{15}$$

where $\lambda_1 = r_b/r_o$, $\lambda_2 = r_b/x_c$ and $\lambda_3 = \lambda_2/2\lambda_1$. The multipole method is used, for example, in Earth Energy Designer (EED) software for calculating the thermal resistance of grout material.

Sharqawy et al. (2009) also proposed an alternative method to evaluate the thermal resistance of grout. They used a 2-dimensional numerical model to validate the following equation with the numerical results they obtained:

$$R_g = \frac{1}{2\pi\lambda_g}\left[-1.49\left(\frac{2x_c}{D_b}\right) + \right.$$

$$\left. 0.656\ln\left(\frac{D_b}{D_p}\right) + 0.436\right], \qquad (16)$$

where D_b the borehole diameter and D_p is outer pipe diameter. They noticed that the maximum error occurring between the numerical and theoretical resistance calculated with equation (16) was only 5%.

3.3 Borehole thermal resistance

The thermal resistance of the borehole and the thermal conductivity of the surrounding subsurface are the two main parameters, in addition to the undisturbed initial temperature of the bedrock, when optimizing the required length of the BHE. The thermal resistance can be evaluated experimentally using the conventional or distributed thermal response test or with the theoretical equations presented in Chapters 3.1 and 3.2, although these usually overestimate the true borehole thermal resistance. It has been experimentally proven that the borehole thermal resistance obtains its largest value when the pipes are close to each other and near the borehole center. In this case, the temperature difference between fluid average and borehole wall temperature is large and heat transfer between pipes reduces the efficiency of the system. Borehole thermal resistance R_b consists of three components, which are the resistance of the circulating fluid inside the polyethylene pipes, R_f, the thermal resistance of the pipe material, R_p, and the resistance of the borehole filling material, R_g.

Fluid thermal resistance R_f is usually neglected in borehole thermal resistance calculations, because it is much lower than that of the pipe or borehole filling material due to the turbulent flow conditions and high convective heat transfer coefficient. In a stationary state, heat flux from the heat carrier fluid to the inner pipe surface must be the same as that between inner and outer pipe surfaces (Incropera & Dewitt 2002). Hence, if materials are connected in a series, the total thermal resistance between different materials can be calculated as a sum of individual resistances, i.e.

$$R_{tot} = R_1 + R_2 + \cdots + R_n. \qquad (17)$$

On the contrary, if materials are connected in parallel, the total resistance R_{tot} can be evaluated from the equation

$$\frac{1}{R_{tot}} = \frac{1}{R_1} + \frac{1}{R_2} + \cdots + \frac{1}{R_n}. \qquad (18)$$

Borehole thermal resistance can be thought of as a combination of series and parallel circuits in such a way that total resistance is

$$R_b = R_g + \frac{1}{\frac{1}{R_{ig}} + \frac{1}{R_{og}}}, \qquad (19)$$

where R_{ig} is the thermal resistance between the fluid in inlet pipe and the outer pipe radius (Al-Khoury 2012). If one assumes that the thermal resistance between the ascending shank and borehole wall is the same as that between descending shank and borehole wall ($R_{ig} = R_{og}$), and the pipes are positioned symmetrically in the borehole, the borehole thermal resistance can be calculated from the equation

$$R_b = R_g + \frac{R_{ig}}{2}, \qquad (20)$$

where R_{ig} is the sum of resistances R_f and R_p. This Y-configuration circuit disregards the internal thermal resistance between descending and ascending shanks, thus assuming that heat flux from the heat carrier fluid to the surrounding rock or vice versa is the same for both pipes.

4 ANALYTICAL INTERPRETATION OF THERMAL RESPONSE TESTS

When planning a large borehole heat exchanger system (BHES), ground thermal properties such as thermal conductivity and volumetric heat capacity are needed as simulation input parameters to estimate the necessary borehole depth and number of boreholes. The thermal response test offers a good way to estimate parameters having an effect on the heat transfer efficiency. The sizing of the borehole field without measured properties may be unreliable, since it may be under- or overestimated,

and there might thus be an insufficient number of boreholes in the field. The thermal response test also offers a good way to determine possible groundwater movements near the borehole, since it has a direct impact on the effective thermal conductivity of the bedrock. Results from TRT measurements can be interpreted by either numerical or analytical methods. In this chapter, we examine the analytical infinite line source method for describing heat transfer from the borehole to the surrounding soil. The two most commonly used methods for TRT interpretation are the infinite line source (ILS) and cylinder source (ICS) methods. In the experimental analysis, we use the line source method combined with temporal superposition, which takes into account variations in the heat power injected into the bedrock.

The usual practice with the conventional thermal response test is to log the fluid inlet and outlet temperatures during the heat injection period. Thus, bedrock thermal conductivity and borehole thermal resistance must be calculated using only heat injection data. Recent research, however, has revealed that the thermal recovery period provides the best information on the bedrock thermal conductivity. This is because radial temperature gradients in the borehole are low and borehole thermal resistance is zero during recovery, since there is no heating during this phase (Acuña 2013). Temperatures between the borehole wall and heat carrier fluid match reasonably well when the heater unit in the TRT rig is switched off. Since there is no temperature difference between the working fluid and the borehole wall, the borehole thermal resistance cancels out. Therefore, the fluid temperature inside the pipe does not depend on the fiber location during the recovery period.

4.1 Infinite line source method

Because the relationship between borehole depth and diameter is very strong, the infinite line source method provides a good and reliable way to evaluate temperatures at different radiuses from the heat source. The combination of the borehole and pipes must be assumed as a long linear heat source that injects or extracts heat with a constant heat flux. The temperature of the surrounding bedrock can be calculated at any time point and distance from the heat source. Heat is conducted from the line source to the ground or vice versa only in a radial direction normal to the line source length in a homogeneous and isotropic soil formation. The thermal conductivity of the bedrock in a particular layer is thus uniform. Two important assumptions considering the line source method are that the temperature of the surrounding bedrock at an infinite distance from the heat source does not change with time, and the undisturbed initial temperature of the system is the same everywhere.

The infinite line source method is the most commonly used analytical solution for considering the conductive heat transfer in a medium. It is derived from the heat equation, which defines how efficiently or poorly heat is transferred and stored in a specific material. The heat equation is written in Cartesian coordinates as

$$\rho C_p \frac{\partial T}{\partial t} = \nabla \cdot (\lambda \nabla T) + Q_{gen}, \qquad (21)$$

where T [K] is the subsurface temperature and Q_{gen} [W/m³] is the heat generated in the system (Incropera & Dewitt 2002). The energy balance between different materials can be presented using a general heat equation that takes into account both heat conduction and convection. The general assumption is that heat is only transferred in the radial direction, thus eliminating the vertical effects occurring between the ground surface and the bedrock. This assumption is only valid if the subsurface geothermal gradient is small.

When the far field temperature of the surrounding bedrock is assumed constant at an infinite radius from the heat source, i.e. (r = ∞, t) = T_0, then the temperature difference for a homogeneous and isotropic medium at a radius r and time t is

$$\Delta T(r,t) = \frac{Q}{4\pi\lambda L} \int_s^\infty \frac{e^{-s}}{s} \, ds, \qquad (22)$$

where s = r²/(4αt) and thermal diffusivity α=λ/(ρC_p) (Marcotte & Pasquier 2008). Equation (22) is usually approximated with the first two terms of the Taylor series regarding the exponential integral as

$$\Delta T(r,t) = \frac{Q}{4\pi\lambda L} \left[\ln\left(\frac{4\alpha t}{r^2}\right) - \gamma \right]. \qquad (23)$$

Equation (23) does not provide an exact solution to the exponential integral (Monzó 2011), but it has been shown that the logarithmic definition is valid and has good accuracy when the following time criterion is true

$$t > \frac{5r^2}{\alpha} = \frac{5\rho C_p r^2}{\lambda}.\tag{24}$$

Usually, the first 10–15 hours of TRT heat injection data are disregarded, and only later time data are used when solving the thermal parameters. The accuracy improves as time evolves, because heat is no longer stored in the groundwater and rock formation close to the line source. Thermal diffusivity defines how rapidly a heat pulse proceeds in the bedrock. If the volumetric heat capacity of the bedrock is low and thermal conductivity high, a heat pulse moves effectively through the rock formation. Conversely, if the volumetric heat capacity is large and the borehole thermal parameters are evaluated using data immediately after the heat transfer has begun, we measure grout parameters and not those of the bedrock.

In the conventional thermal response test, temperature probes (PT-100, thermocouples, or DTS) continuously measure fluid temperatures at the ground surface. The borehole thermal resistance can be calculated as the difference between the average temperature of the heat carrier fluid, T_f, and the borehole wall temperature, T_w, using the equation

$$R_b = \frac{[T_f(t) - T_w(t)]L}{Q(t)},\tag{25}$$

where L is the borehole length and Q the injected heat flow into the borehole during TRT measurement. The theoretical average temperature of the heat carrier fluid is therefore

$$T_f(t) = T_w(t) + \frac{Q(t)}{L}R_b.\tag{26}$$

Since the temperature at the borehole wall is $T_w(t) = T_0 + \Delta T(r_b,t)$, the mean heat carrier fluid temperature can be obtained from the equation

$$T_f(t) = T_0 + \frac{Q}{4\pi\lambda L}\left[\ln\left(\frac{4\alpha t}{r_b^2}\right) - \gamma\right] +$$

$$\frac{Q}{L}R_b = \frac{Q}{4\pi\lambda L}\ln(t) + C,\tag{27}$$

where rock thermal conductivity λ and borehole thermal resistance R_b are unknown and solvable parameters, and T_0 is the undisturbed initial temperature of the bedrock. Equation (27) can be used to solve the rock thermal conductivity and borehole thermal resistance when the heat flux injected into the ground is nearly constant. When plotting the measured average temperature of the heat carrier fluid against the natural logarithm of time, one can solve the bedrock thermal conductivity from the equation

$$\lambda = \frac{Q}{4\pi Lk},\tag{28}$$

where k is the slope of the line fitted to the experimental temperatures. During a stationary case, the injected heat flux is constant and the average fluid temperature rises linearly, and the term C in the line source equation (27) is not time dependent. The borehole thermal resistance can be solved once the soil thermal conductivity is known. In this study, we used the least squares fitting method with equal weighting to iteratively find the best values for bedrock thermal conductivity and borehole thermal resistance so that the error between the measured and calculated average fluid temperature would be as small as possible.

The total heat power Q injected into the soil and rock during the conventional thermal response test is calculated using the volumetric flow rate ($\dot{V}$), volumetric heat capacity (ρC_p), and the temperature difference between inlet and outlet at the ground surface, i.e.

$$Q(t) = \rho\dot{V}C_p\Delta T(t).\tag{29}$$

When using the heat power value calculated with Eq. (29) in the line source equation, one obtains as a result the average thermal conductivity along the total borehole length. The borehole is thus only divided into one layer with a length that is the same as the borehole depth.

In a distributed thermal response test, heat transferred into the rock in a specific layer is calculated with four temperature values located in the top and bottom of each particular layer according to Figure 3. The flow direction in the pipes is indicated with red and blue arrows, and since the temperatures of the descending flow during the heat injection phase are higher, i.e. T1 > T2 > T3 > T4, the heat rate for a particular layer can be calculated with the following equation:

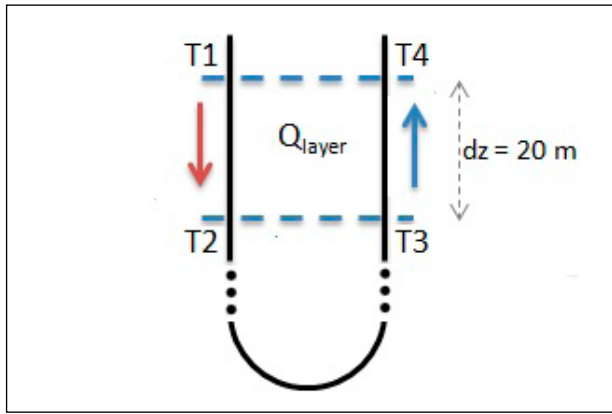$$Q_{layer} = \rho C_p\dot{V}(T1 - T4 - T2 + T3)\tag{30}$$

Fig. 3. Heat rate calculation in a Distributed Thermal Response Test. Photo: Petri Hakala, GTK.

4.2 Superposition technique

The infinite line source method presented in Chapter 4.1 is only valid when the injected heat flux remains constant over the whole heating period in the thermal response test. If there are large variations in the heat power, the constant power assumption will not be valid. The line source method can be used if variable heat injection rates are taken into account with the superposition technique, which means that heat power is divided into several pulses with a constant heat rate and the same time step. If the heat rate increases or decreases during the heating period, the constant heat rate assumption may distort the results. If the distributed thermal response test consists of both heating and recovery periods, there is change in the heat power immediately after the heating period. This is why a temporal superposition method must be used. In accordance with the superposition principle, the total heat rate is divided into several pulses based on the following equation (Monzó 2011):

$$q(t) = \begin{cases} q_1, & t_0 = 0 < t < t_1 \\ q_2, & t_1 < t < t_2 \\ q_n, & t_{n-1} < t < t_n \end{cases} \tag{31}$$

Figure 4 presents the concept of temporal superposition in a graphical form. First, the heat pulse q_1 applies for the whole time period t_n and all the following pulses are superposed with the initial pulse. The exponential integral in the line source equation $\left(E_1(s) = \int_s^\infty \frac{e^{-s}}{s} \, ds \right)$ can be evaluated with the infinite Taylor series as

$$E_1(s) = \left[-\gamma - \ln(s) + \sum_{i=1}^{n} (-1)^{i+1} \frac{s^i}{i \cdot i!} \right], \tag{32}$$

where γ is the dimensionless Euler constant, the numerical value of which is 0.5772 (Raymond

et al. 2011). As noted earlier in Chapter 4.1, the Taylor series provides a good approximation of the exponential integral with just the first two terms of the series.

After the heat rate is divided into several pulses, the average fluid temperature can be calculated using the infinite line source method as (Raymond et al. 2011)

$$T_f(t) = T_0 + q_i R_b + \sum_{i=1}^{n} (q_i - q_{i-1}) \frac{E_1(s)}{4\pi\lambda}, \tag{33}$$

where the parameter s takes into account what happens in the different time periods during the distributed thermal response test. It depends on the time difference between adjacent heat pulses and subsurface thermal diffusivity according to the equation (Raymond et al. 2011)

$$s = \frac{r_b^2}{4\alpha(t - t_{i-1})}. \tag{34}$$

If one wants to calculate the fluid average temperature, for example, at time point $t_2 < t < t_3$ (see Fig. 4), three different heat pulses are used and temperature obtains the value

$$T_f(t) = \frac{q_1}{4\pi\lambda} E_1 \left(\frac{r_b^2}{4\alpha(t - t_0)} \right) +$$

$$\frac{q_2 - q_1}{4\pi\lambda} E_1 \left(\frac{r_b^2}{4\alpha(t - t_1)} \right)$$

$$+ \frac{q_3 - q_2}{4\pi\lambda} E_1 \left(\frac{r_b^2}{4\alpha(t - t_2)} \right) + q_3 R_b + T_0. \tag{35}$$
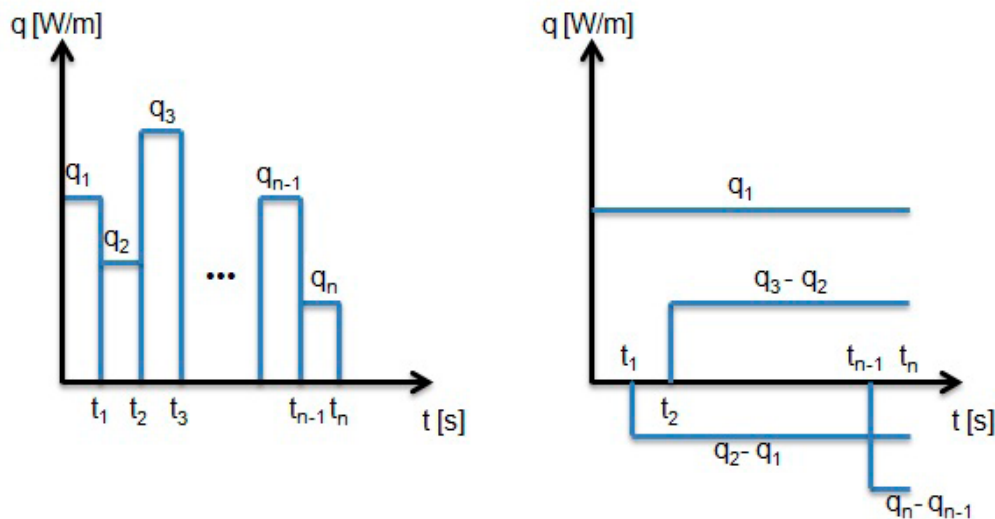
Fig. 4. Heat power divided into n heat pulses according to the temporal superposition technique. Photo: Petri Hakala, GTK.

If there is no difference between adjacent heat pulses, i.e. $q_1 = q_2 = \cdots = q_n$, then superposition equation (33) minimizes back to the constant infinite line source equation (27).

5 THE DTS device and fiber configuration used in DTRT measurement

5.1 Distributed temperature sensing (DTS)

Distributed temperature sensing can be used in many applications such as monitoring pipelines, power cables and oil/gas wells. It is probably most useful in fire detection in tunnels and large buildings. Although the monitoring cable will be damaged by fire or other hazardous actions, the temperature sensing can be continued and the cutting point can be detected. In research applications, it can also be used in various important measurements, because the temperatures are collected from the whole length of the cable, and up to thousands of temperature points may be recorded at the same time in a few minutes.

Distributed temperature sensing is based on Raman back scattering in a fiber optic cable. The laser light is always scattered because of the distortions in the optical fiber glass. Low intensity scattering mostly occurs by Rayleigh (elastic), Brillouin, and Raman scattering (both nonelastic). The wavelength of the monochromatic light sent by the laser is shifted to Stokes and anti-Stokes backscatter. Stokes scattering is reflected in longer wavelengths, and its amplitude is not temperature dependent. In contrast, the shorter wavelength anti-Stokes amplitude is temperature dependent. With the Stokes and anti-Stokes amplitude ratio, temperatures can be determined at the scattering point. The distance over which the light is back scattered is very accurately defined by the measurement time. As the time of sending a laser pulse is known, the only parameter to measure is the back-scattering time. The laser travels at the speed of light in the fiber, and the time is only a few nanoseconds at a distance of one meter. The performance of the DTS device for spatial resolution is dependent on the ability to measure time (Selker et al. 2006a, Selker et al. 2006b).

The DTS uses the fiber optic cables as a temperature sensor. The fiber type is commonly Graded Index Multimode 50/125 μm fiber. Nowadays, the cables can be specially designed for temperature sensing. These cables are very sensitive to temperature changes and the response time is very short, being about 10 seconds. The DTS measurements can be performed using single- or double-ended configurations. With double-ended measurements as a U-shape, the signal returns to another DTS channel, from where the signal is sent back in the opposite direction. Double-ended measurement is more accurate than single-ended measurement and the number of calibration functions is smaller. In any case, each DTS measurement requires calibration. Double-ended measurement only requires offset calibration at one known temperature

point. In single-ended measurement, calibration of the gain and attenuation is needed together with offset calibration. This calibration requires several temperature points along the cable. After proper calibration, the temperatures can be accurately obtained and a temperature resolution of less than 0.1 °C can be achieved. The measurement time de- pends on the desired spatial resolution. A shorter spatial resolution requires longer measurement times, and vice versa. Accurate DTS devices can measure spatial resolutions of shorter than one meter, and the normal measurement time is 2–10 min for the whole cable. The range of the cables is over 4 km in most DTS devices.

5.2 Dimensions of the studied borehole heat exchanger

Distributed and conventional temperature meas- urements were carried out at a groundwater-filled test borehole located in Espoo, southern Finland. The TRT rig was connected to U-collector pipes and optical fiber cables were placed inside both pipe shanks. Before fluid pre-circulation was start- ed, the undisturbed initial temperature profile of the bedrock was measured with DTS and a min- iaturized temperature data logger device, and the active depth of the borehole was measured. Since the borehole depth was 200 m and the groundwa- ter level was 2.8 meters below the ground surface, the active depth of the borehole was 197.2 m. The borehole diameter was 115 mm and there were no spacers between the polyethylene pipes, mean- ing that pipe locations in the borehole were not known. In the winter, the temperature of the heat carrier fluid inside the pipes might drop below zero degrees, and a mixture of water and ethanol is consequently usually used as a heat carrier fluid, since its freezing point is lower than that of pure water. Pipes were also filled with an ethanol water mixture in the test borehole.

Optical fiber cables were placed inside the poly- ethylene pipes, and fluid temperatures were con- sequently logged along the borehole length in ascending and descending pipe shanks. The bore- hole was divided into 9 layers of 20 meters each, as illustrated in Figure 5. The first and last 10 meters of the borehole were disregarded due to the ambi- ent air influence near the ground surface and dis- turbances of the fiber splicing at the bottom of the borehole.
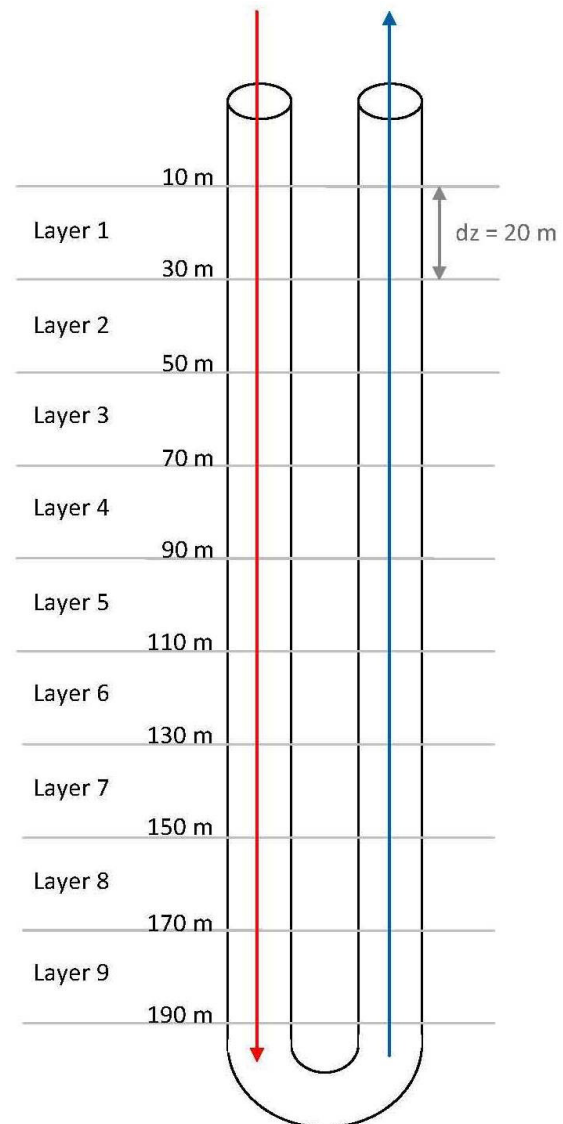

Fig. 5. Multilayered model of the borehole. Photo: Petri Hakala, GTK.

5.3 Fiber configuration in the borehole

The DTS measurement procedure in this study was designed so that the temperatures of the heat carrier fluid from both BHE pipes, the inlet and outlet, could be measured. Both pipes had cables, which were 400 m and 700 m long, respectively, and were fusion spliced together. The cable ends were attached to the DTS instrument with E2000 connectors. The other cable ends at the bottom of the pipes where fusion spliced to other fibers in the cable for double-ended measurements. These
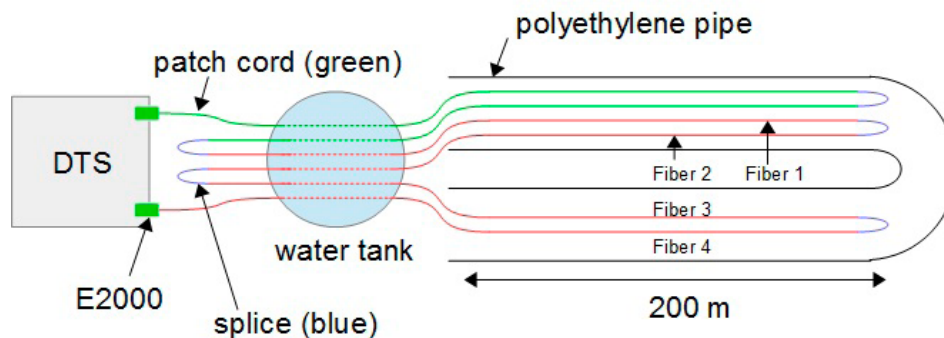
Fig. 6. Fiber configuration between the DTS device and borehole. Photo: Petri Hakala, GTK.

fusion splices were placed in a small tube with a diameter of about 10 mm and glued to make them water resistant (Fig. 7). Because of the small diameter, there was some noise at the bending point. This is why we disregarded the last 10 m of data from the bottom of the pipes. However, the use of fusion splices is still the best way to ensure accurate measurements. We only used connectors in the DTS connection. After each connector or fusion splice, one should have at least one calibration point. In this study, we used a water tank with a volume of approximately 50 dm³ for calibration to reduce the influence of the air temperature (Fig. 6). Each cable had approximately 50 m of cable in the calibration tank. The water temperature in the tank was measured by an autonomous temperature logger. Also it is important to have some extra cable or patch cord after the DTS device, because the laser transmitter is often very powerful and could affect the first measurements. In our experience, it is necessary to have a few hundred meters of patch cord. In this study, we obtained double temperature measurements from both pipes because of the splicing at the bottom of the pipes. We used the first cable lengths from the DTS device as a patch cord. The total length of optical fiber cable used for measurement was 3000 m from the 400 m (4 fiber × 400 m) and 700 m (2 fiber × 700 m) spliced cables. The cable we used was Brugg Cables BRUsens with four fibers in the cable. The cable diameter was only 3.8 mm, thus minimizing the effects on the fluid flow. Fibers 4 and 3 (Fig. 6) were in the 700 m cable and the rest of them were in the 400 m cable. The cables were connected to each other at the point marked "splice (blue)" in Figure 6.

The temperature measurements were performed with an Agilent N4386A DTS device. We used only two channels for double-ended measurement from our four-channel device. We chose to have quite a high spatial resolution of 3 meters to detect possible fissures and cracks. The measurement time was 10 minutes, which was long enough to provide better resolution.

Fig. 7. Distributed temperature-sensing cables (Geological Survey of Finland). Photo: Ilkka Martinkauppi, GTK.

6 DATA FROM NUPURI DTRT MEASUREMENT AND ITS INTERPRETATION

6.1 Geological mapping of the study site

The study site is located in the northern part of the city of Espoo, near Nupurinjärvi, which is between the Turunväylä highway and Nupurintie (Fig. 8). The distance between Helsinki, the capital of Finland, and the test borehole is only about 30 kilometers. The borehole is marked as a green circle on the map. In the area it is planned to build single-family and terraced houses. Entering into the planning process, the utilization of a large ground source heat pump system (GSHP) was examined as an energy source for heating (Leppäharju et al. 2008).

Geologically, the study site is located between a north–south-oriented large fracture zone and a long northwest and southeast diabase vein. Near the lake shoreline, the bedrock is covered with fine-grained sediments such as clays, but the nearby rock is also denudated. While drilling, soya powder samples were collected from the borehole and were analyzed using a scanning electronic microscope (SEM) to evaluate the mineral content. Based on SEM analysis, the granite at Nupuri mainly consists of quartz, K-fsp and albite according to Figure 9. It should be noted that the sampling depth is indicative. The quartz content at the bottom of the borehole is clearly greater than at about 50 meters depth, implying higher thermal conductivity at the bottom of the borehole. The color of the bedrock varies from gray to reddish. (Peltoniemi 1996, Kielosto et al. 2002, Leppäharju et al. 2008).
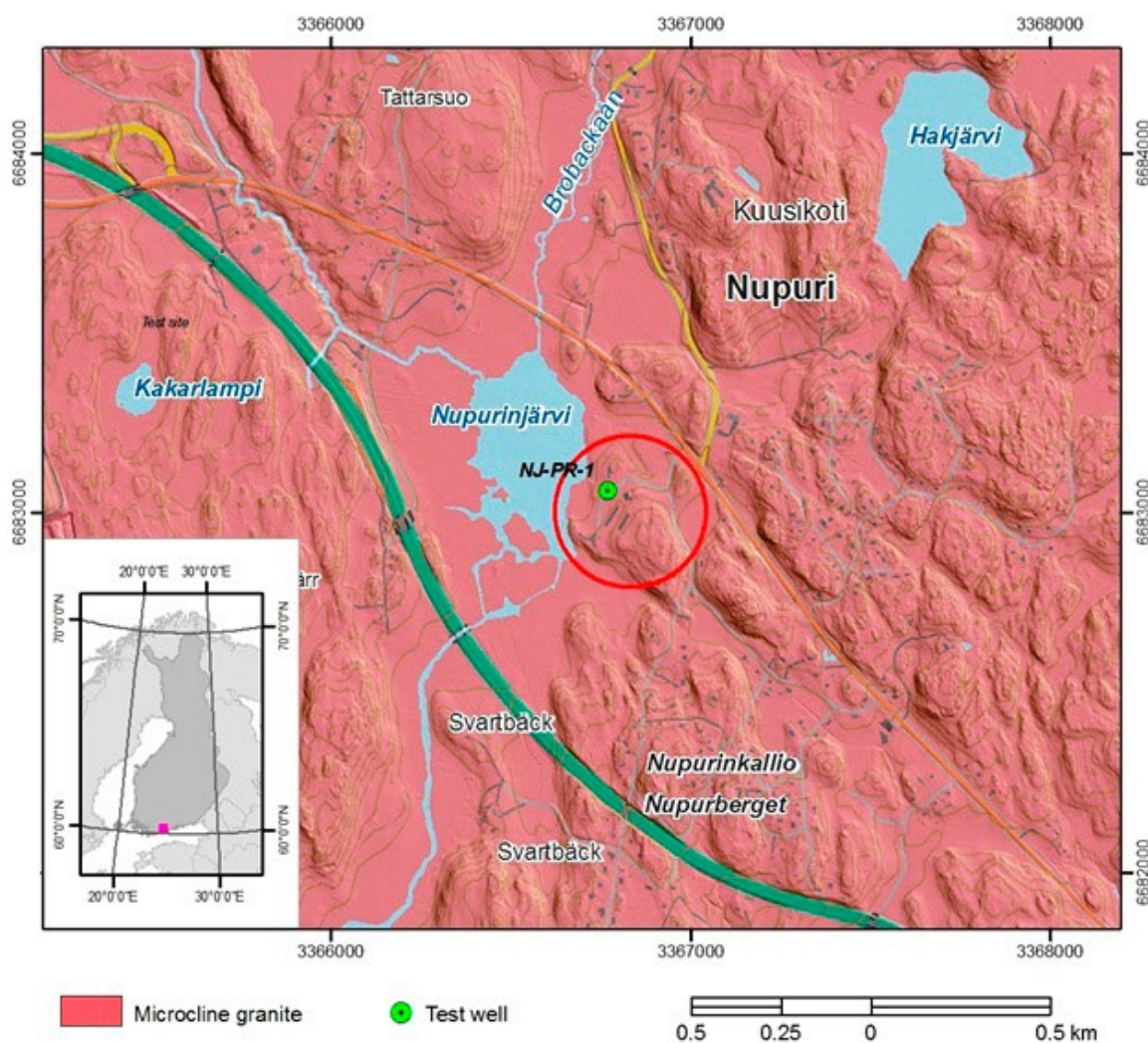

Fig. 8. The geology of the study site. The test well is marked with a green circle. Basemaps: © National Land Survey of Finland, 2013. Geological data: © Geological Survey of Finland. Photo: Annu Martinkauppi, GTK.
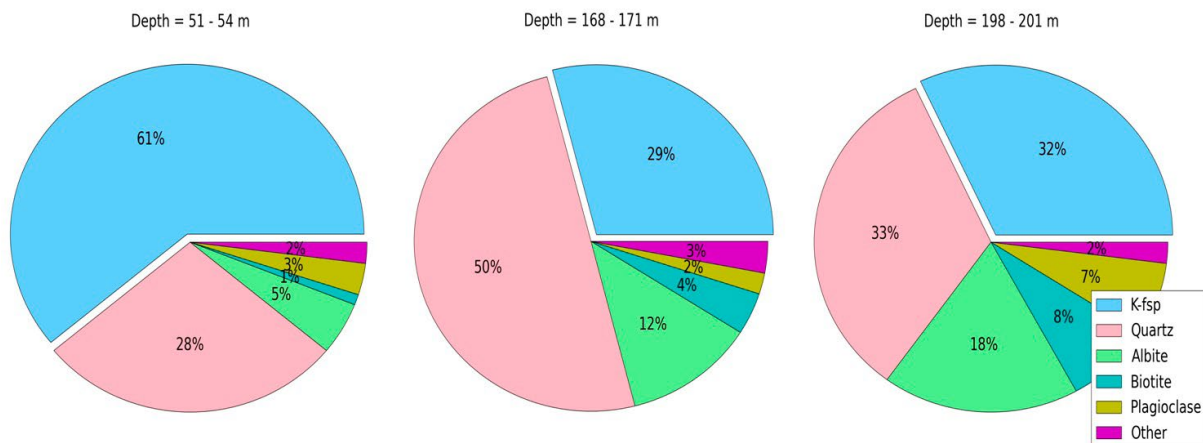
Fig. 9. SEM analysis results from borehole soya powder samples. Photo: Petri Hakala, GTK.

The borehole was optically scanned and possible cracks were analyzed, with a few being encountered (0.92–2.01 cracks per meter at a depth of 2.5–100 m). Cracks were mainly compact and filled with carbonate. Some cracks were clay filled. In geophysical investigations of the borehole, temperature, density, susceptibility, gamma radiation, and the resistivity of the bedrock and water were measured. They all showed the bedrock to be homogeneous and solid, with no notable changes in rock type being detected. Nupurinkallio is probably a solid segment between two fracture zones. (Leppäharju et al. 2008)

6.2 Initial temperature profile of the bedrock

The DTRT test procedure consisted of four separate phases, i.e. the undisturbed phase, pre-circulation, heating, and recovery. The undisturbed temperature profile of the bedrock measured with the DTS device is presented in Figure 10. In total, four optical fiber cables and two patch cord fiber cables (not used in data interpretation) were present inside the U-collector, which is why Figure 10 presents four temperature profiles. Fluid temperatures measured by fiber 1 are somewhat larger than those in fiber 4 at each depth. These variations might be due to the different fiber locations in the pipe shanks, since fibers 1 and 2 were placed in the same pipe and the temperature difference between them was smaller than that between fibers 1 and 4. The distortion in the temperatures is normal when measuring with DTS and using a high spatial resolution (in this case 3 m).

Another typical way to measure the initial ground temperature profile at Geological Survey of Finland is to use an Antares type 1854 miniaturized temperature data logger. This is lowered into the borehole to measure the bedrock temperatures at desired depths. The undisturbed average temperature of the bedrock can also be determined during the pre-circulation phase of the TRT, since fluid temperatures at the inlet and outlet of the U-pipe gradually approach the rock temperature if there is no heating during fluid circulation. Since the bedrock thermal conductivity and borehole thermal resistance were calculated using experimental temperatures measured with the DTS device, the Antares and TRT rig temperature probe values were not analyzed in this report. The TRT rig was used for heating of the heat carrier fluid
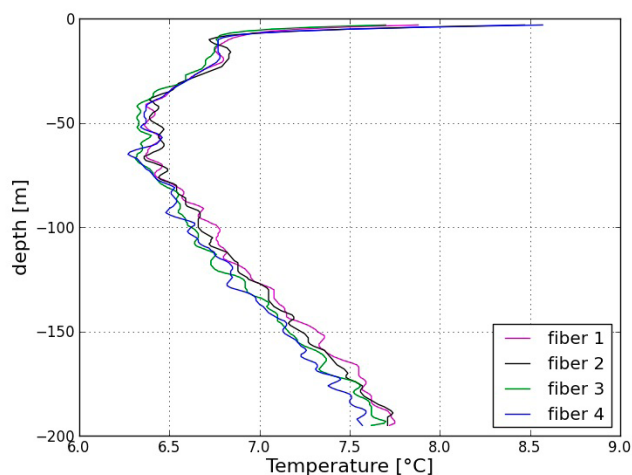

Fig. 10. The undisturbed temperature profile of the bedrock. Photo: Petri Hakala, GTK.

during the heat injection phase with electrical resistances, but all temperature values presented were measured with the DTS, although the rig also contains four temperature probes for fluid temperature calculation.

The bedrock geothermal gradient determined from DTS temperature data, between the depth intervals of 60–200 m, was approximately 1.1 ºC/100 m, i.e. after 60 meters, the bedrock temperature rises by approximately 1.1 ºC per 100 meters. In the pre-circulation phase, an ethanol/water mixture was circulated in the pipes for about one hour. The volumetric flow rate of the heat carrier fluid was approximately 48.75 l/min. When the temperature difference between the inlet and the out-

let was small enough, three electrical resistances (each 3 kW) in the TRT rig were switched on and temperatures at different depths were logged for about 94 hours, i.e. during the whole heat injection period. The recovery period started immediately after 94 hours of heating, meaning that electrical resistances in the TRT rig were switched off, as was fluid circulation, but fluid temperatures were measured using the DTS device in each layer at one-meter intervals for about 216 hours. This was not long enough for total thermal recovery to the initial undisturbed bedrock state, as can be seen in the next chapter. Overall, measurement took about 310 h, heat injection lasted 94 h and recovery 216 h.

6.3 Average fluid temperature during heat injection and recovery phases

Figure 11 presents the average fluid temperature measured in the heat injection and recovery phases. As can be seen, the temperature measured using equation (1) with the inlet and the outlet values at the ground surface (blue line) do not exactly describe the true average temperature of the fluid (red line) during the heating period. The same phenomenon is even more clearly observed in the recovery period beginning at the 94 h time point. The true average temperature is measured as the arithmetic mean of all temperature values in fiber 1 and fiber 3, which represents temperatures in the descending and ascending flows (likewise in the fiber couple 2 and 4, respectively). Since the depth

of the borehole was 200 meters and fluid temperatures were measured at one-meter intervals from both pipe shanks, the true average temperature of the fluid was calculated using 400 temperature values at each time point. During the recovery period (no fluid circulation), the red temperature profile in Figure 11 represents the average bedrock temperature along the whole borehole length, and the blue line the ground surface temperature only. This is why the blue line temperature cannot be used to calculate the bedrock thermal conductivity from the recovery period, since it does not represent the bedrock temperature. In Figure 11, almost consistent diurnal temperature variation can be seen in both temperature curves. Variation is natural when the temperature is measured at the ground surface. However, diurnal temperature variation measured with optical fiber cables is assumed to derive from the DTS device, which was exposed to the air temperature variations. The same phenomenon is also seen in Figure 12.

The thermal conductivity of the bedrock and thermal resistance of the borehole can be calculated from the temperature data presented in Figure 11. Acquired results (conductivity and resistance) conventionally only describe the average values for the bedrock surrounding the borehole. In order to calculate parameters for individual layers, the average fluid temperature in each layer must be known. In this report, the borehole was divided into nine layers, each 20 meters thick (first layer between 10–30 m and the last between 170–190 m), and average fluid temperatures were defined separately for each layer. Measured average tem-
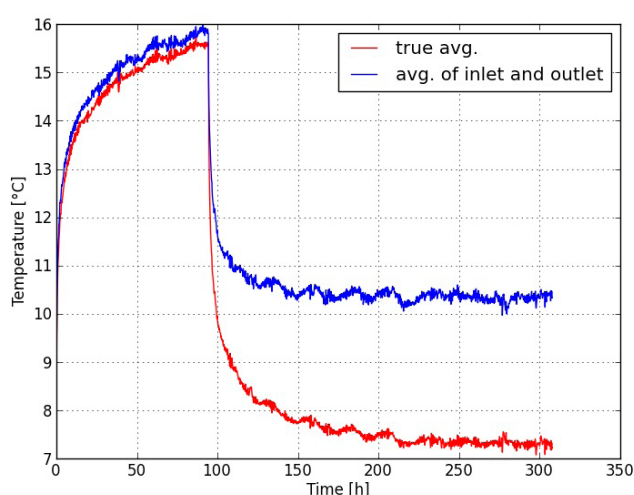

Fig. 11. Average fluid temperatures. The blue line is the temperature measured from the inlet and the outlet section of the BHE at the ground surface level, while the red line is the true average temperature of the fluid measured with the DTS device along the total length of the BHE. Photo: Petri Hakala, GTK.

a) Heating and recovery phase   b) Recovery phase 100–300 hours (zoomed)
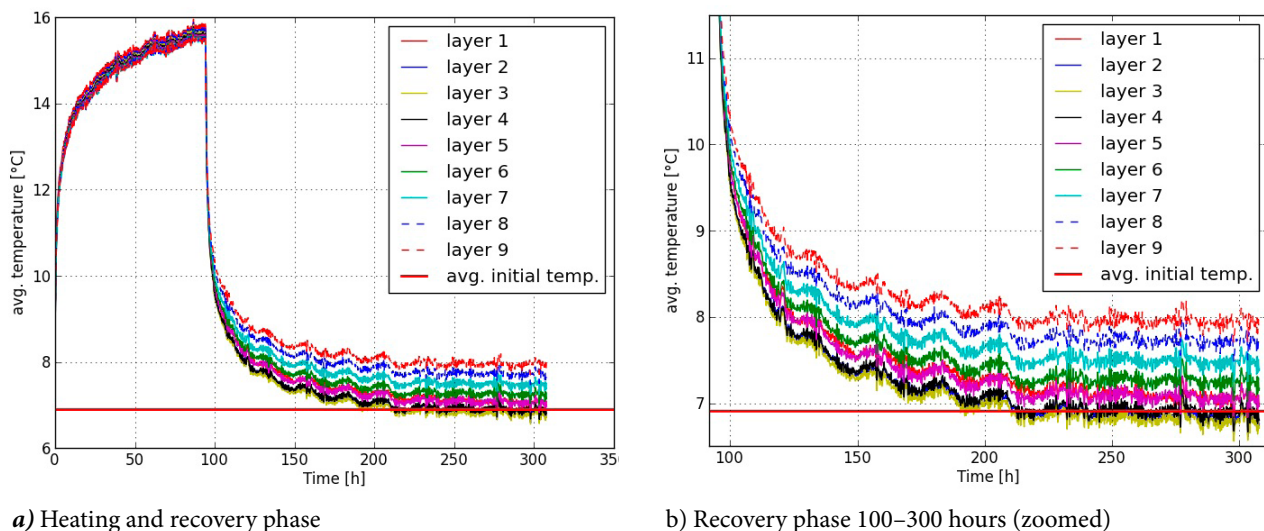
Fig. 12. The temperature profile of each layer. Differences between average fluid temperatures in separate layers are more obvious in the recovery phase than in the heating phase. The average initial temperature of the BHE is marked with a solid red line. Photo: Petri Hakala, GTK.

perature values in each layer are presented in Figure 12. Differences in the temperatures between layers are more obvious in the recovery phase (Fig. 12a) than in the heating phase. The average temperature of the heat carrier fluid was calculated from six temperature values, i.e. three in each pipe within each layer (points located at the top, middle and bottom). The undisturbed initial temperature in each layer was calculated as the arithmetic mean of all measured temperature values in the specific layer. The thermal resistance in groundwater-filled boreholes depends on the injected heat power during the thermal response test. The higher the groundwater temperature is, the larger will be the influence of natural convection. Borehole thermal resistance therefore depends on the groundwater temperature (Gustafsson & Westerlund 2010).

Recovery data profiles at different time points, i.e. 1, 4, 10, 24, 48, 72 and 210 hours after stopping the heating phase, are presented in Figure 13. The bedrock temperature gradually approaches

the undisturbed initial state, although recovery is clearly more rapid in the early stages than at later times, as can be seen from Figure 13.
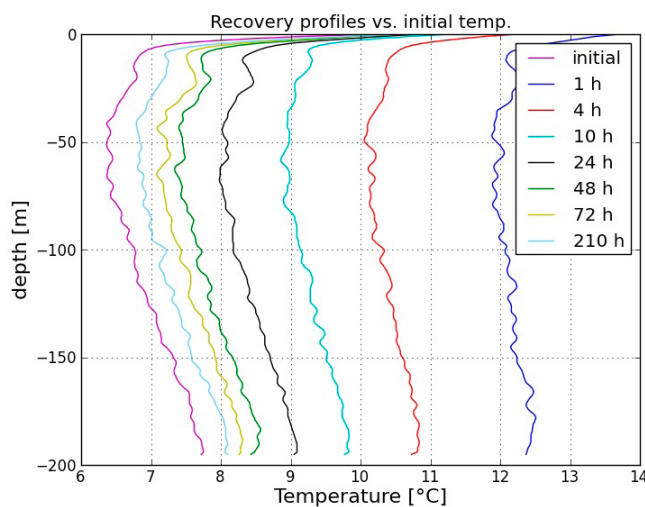

Fig. 13. The temperature profiles following the heating phase, i.e. recovery profiles vs. undisturbed initial temperature. Photo: Petri Hakala, GTK.

6.4 Conventional thermal response test

Bedrock thermal parameters are typically estimated with the infinite line source method (the line source equation (27)), because it is accurate and easy to use. We fitted average fluid temperatures calculated with the line source method to measured temperatures by optimizing the rock thermal conductivity and borehole thermal resistance, minimizing the difference between measured and

calculated temperatures in the different fitting periods. When using the data from the conventional thermal response test, the effective thermal parameters of the bedrock are evaluated from the heating period, and heat carrier fluid temperatures are only logged in the inlet and the outlet section of the BHE. If the DTS device is utilized, the average temperature can also be determined as a true
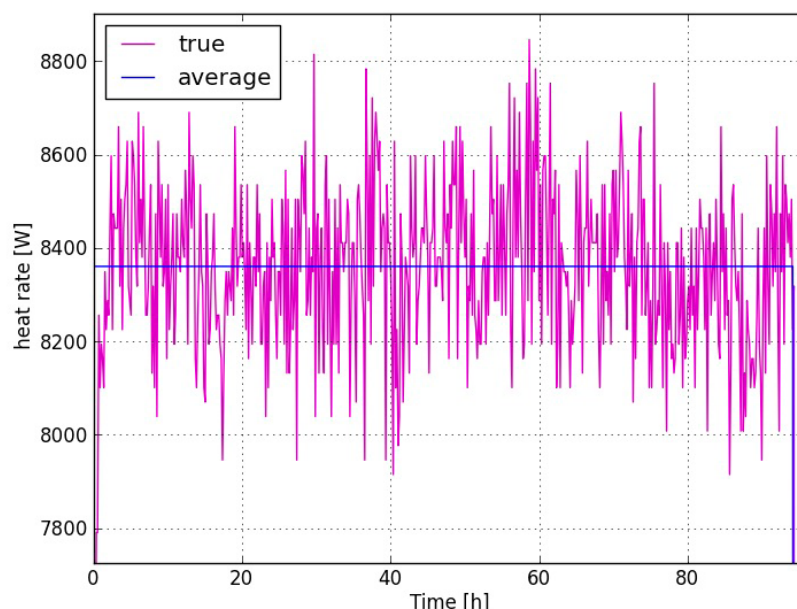
Fig. 14. Variation in the heat power during the heating phase. Photo: Petri Hakala, GTK.

value representing fluid temperatures at different depths.

Variations in the heat power (calculated using inlet and outlet temperature values) during the heat injection phase are presented in Figure 14. The heat power was zero in the recovery phase, since there was no fluid circulation and electrical resistances in the TRT rig were switched off. The average heat power was slightly below 8400 W.

Figure 15 presents the best-acquired fit between measured and calculated average fluid tempera-

tures when the measured average temperature is logged just between the inlet and the outlet of the BHE. Recovery data are disregarded and infinite line source (ILS) optimization is only carried out for the heating period from 10 h to 90 h. When using the ILS equation and assuming constant heat power, according to Figure 14 (blue line), a result of 3.53 W/(m·K) is obtained for the thermal conductivity of the rock and 0.083 m·K/W for thermal resistance of the borehole. However, since the heating rate was not truly stable, varia-
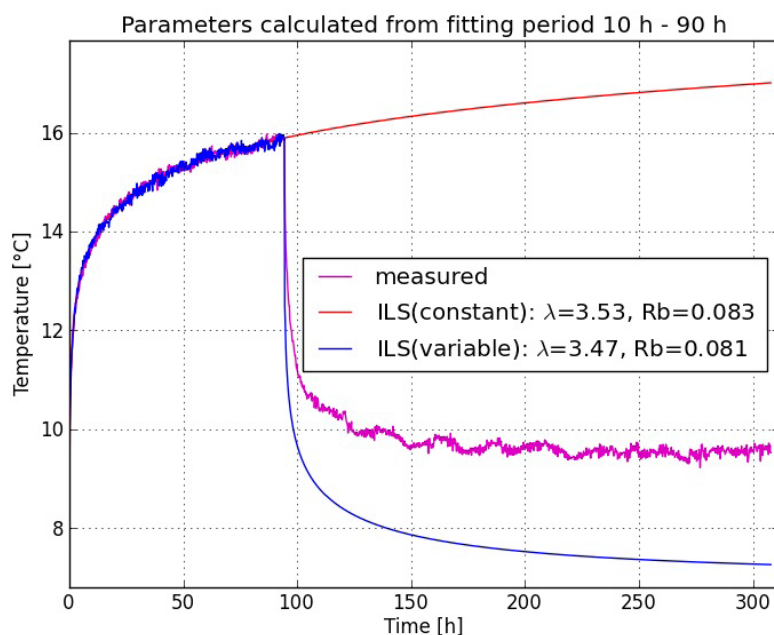

Fig. 15. Best-acquired fit between measured and calculated fluid average temperatures when the measured average temperature is logged just between the inlet and the outlet section of the borehole. Line source optimization is only carried out for the heating period from 10 h to 90 h. Note that the recovery data are disregarded. Photo: Petri Hakala, GTK.
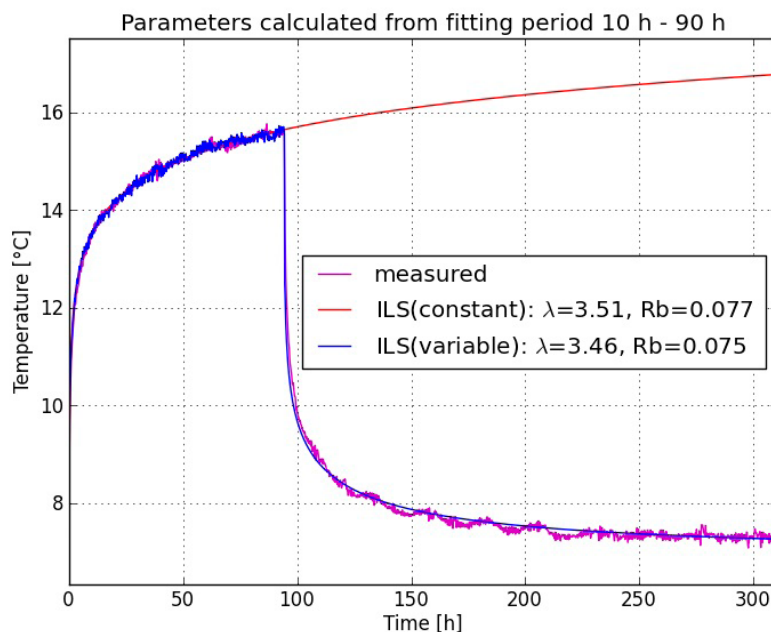
Fig. 16. Best-acquired fit between measured and calculated average fluid temperatures when fitting was carried out using a true average fluid temperature consisting of all measured temperatures at each depth. The figure presents the corresponding fit for the same heating period as in Figure 15. Photo: Petri Hakala, GTK.

tions (magenta line in Figure 14) were taken into account with the superposition technique. The average fluid temperature calculated with equation (33) was fitted with the experimental temperature by adjusting the thermal conductivity of the bedrock and thermal resistance of the borehole until the difference between measured and calculated temperature values in the fitting period was small enough. The results demonstrated that the constant heat power assumption was valid, since values calculated with temporal superposition were 3.47 W/(m·K) and 0.081 m·K/W, respectively, i.e. the differences were negligible between the use of a constant or variable heat rate.

Figure 16 presents the corresponding fit for the same fitting period (10 h to 90 h), but the average fluid temperature at each time point was calculated using 400 temperature values, i.e. representing the true average fluid temperature measured by optical fiber cables. In this case, differences between thermal parameter values are also small depending on which power constant or variable was used. The bedrock thermal conductivity varied between 3.46–3.51 W/(m·K) and the borehole thermal resistance between 0.075–0.077 m·K/W, as can be seen from Figure 16. However, when comparing Figures 15 and 16, it appears that the variable heat rate assumption gives slightly smaller parameter values compared with the constant heat rate assumption.

The bedrock thermal conductivity calculated with the conventional TRT procedure is then approximately 3.50 W/(m·K) and the borehole thermal resistance 0.08 (m·K)/W, regardless of how the average fluid temperature was calculated, i.e. as a true average or mean of the inlet and the outlet section of the BHE. However, since the average fluid temperature determined with the inlet and the outlet of the BHE during the heat injection phase is somewhat higher than the true average temperature, this also directly refers to the borehole thermal resistance. The higher the average temperature of the fluid is, the higher will be the resistance of the borehole, if rock thermal conductivity is the same regardless of how the average fluid temperature was calculated.

6.5 Thermal conductivity determination for separate layers from heat injection and recovery data

Thermal parameter values representing the average value of the whole bedrock surrounding the borehole and borehole itself were presented in chapter 6.4. The average thermal conductivity bedrock was determined as 3.50 W/(m·K) and borehole thermal resistance as 0.08 m·K/W. However, these
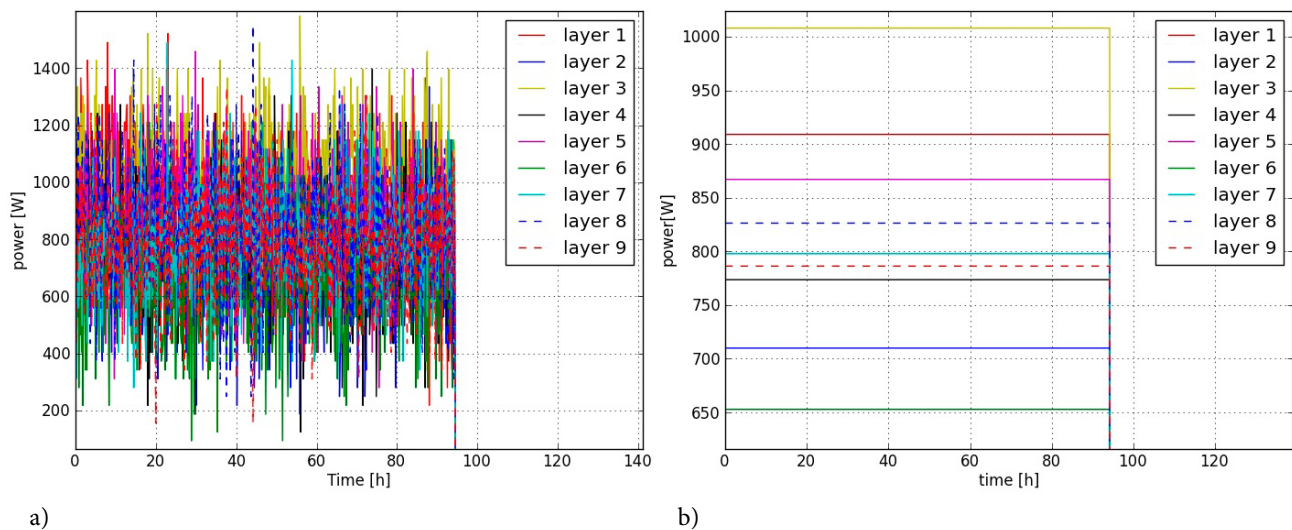
Fig. 17. a) Heat power in each layer. b) Averaged thermal powers over the whole heating period. Photo: Petri Hakala, GTK.

values tell nothing about how heat moves within different layers in the bedrock. Consequently, this chapter presents results acquired from the distributed thermal response test, which directly indicates the differences between layers.

Because there is change in heat power between the heating and the recovery period, it must be taken into account with a superposition principle. The heat power in each layer was calculated according to equation (30). Acquired results are presented in Figure 17(a). Due to temperature fluctuations, heat rate values at different time points differ quite notably. This is why thermal powers were averaged over the whole heating period according to Figure 17(b). As thermal conductivity correlates with heating power, the differences in bedrock thermal conductivity between layers will be visible in Figure 17(b). The heat rate obtains its maximum value in layer 3, therefore indicating the highest thermal conductivity. In layers 2 and 6, heat conducts poorly into the bedrock, and the thermal conductivity in these layers is thus low.

Because of the disturbances in the layered heat power, as was seen in Figure 17(a), the heat rate was divided into several ten-minute pulses, so that during the heating period the thermal power in each step was the same as the average power during the whole heating period. During the recovery phase, there was no fluid circulation, i.e. the thermal power was zero.

If the heat carrier fluid is circulated in the pipes during the recovery period, the bedrock thermal conductivity cannot be determined in separate layers from the recovery data, since the fluid tempera-

ture approaches the average bedrock temperature and not the layer temperature at a specific depth. However, the average thermal conductivity representing the whole borehole can be calculated from the recovery data if the circulation is continued after the heating period. During the recovery phase, the borehole thermal resistance is zero, because there is no temperature difference in the radial direction between the working fluid and the borehole wall, i.e. after heat injection is stopped, the borehole temperature rapidly homogenizes. Temperatures measured during the recovery period are therefore independent of the borehole thermal resistance, and the only parameter that can be calculated from the recovery data is the bedrock thermal conductivity. This acquired conductivity is then used as an input parameter when solving the borehole thermal resistance from the heating data. The borehole thermal resistance is evaluated for the heating period from 10 h to 90 h, and thermal conductivity for the heating period 10 h to 90 h and the recovery period 105 h to 145 h. During the heating period, the unknown positions of fiber cables inside the pipes may have some influence on the measured temperatures. This is one reason why thermal conductivity determination from recovery data is more reliable than in the case of heating data.

Figures 18 and 19 present the thermal conductivity of the rock in different layers calculated from the heating period versus the recovery period. Using the infinite line source method with a constant heat rate assumption, the thermal conductivity is calculated from the fitting period 10 h to 90 h. For example, in layer one, the rock thermal conduc-
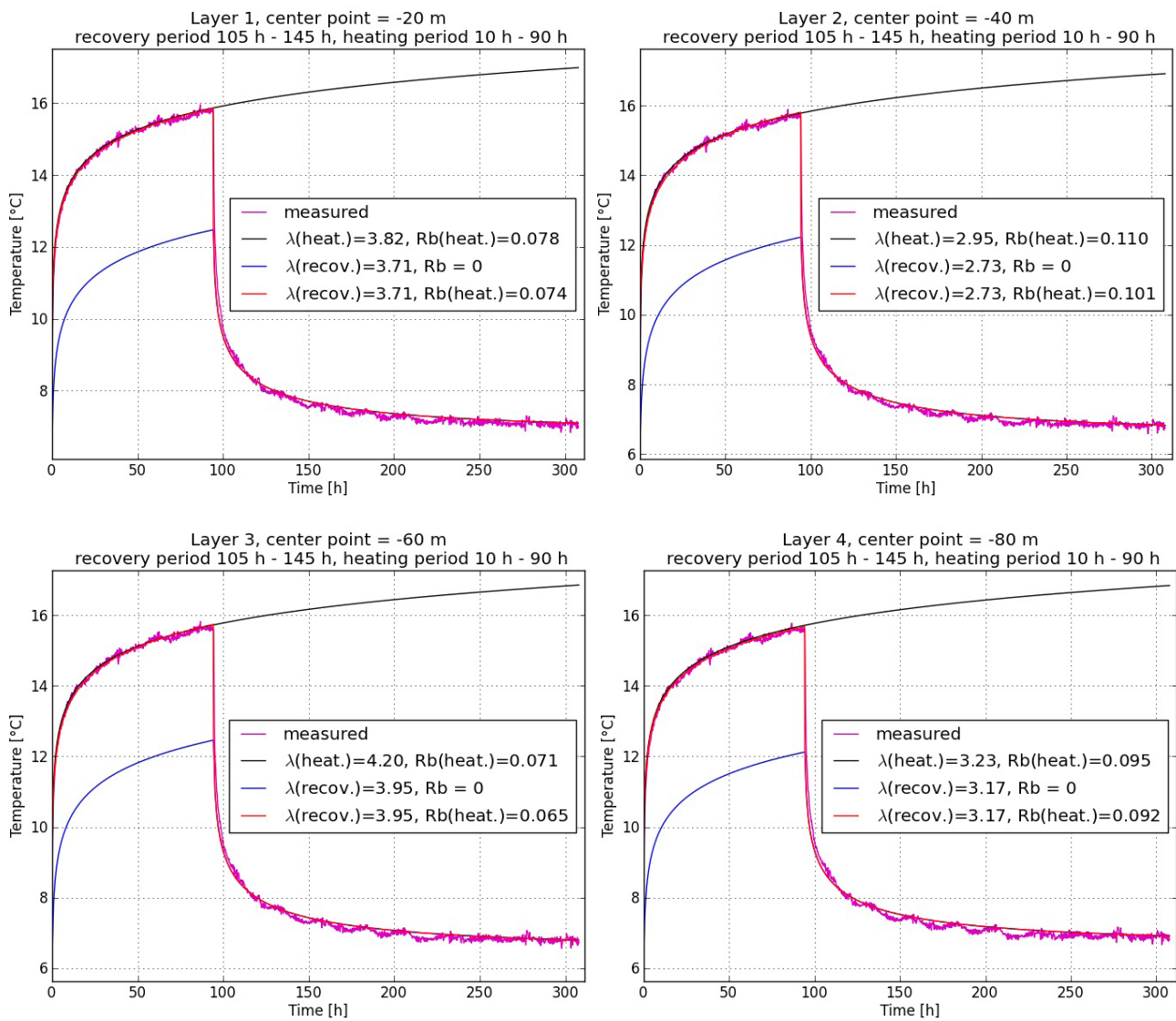
Fig. 18. Rock thermal conductivity and borehole thermal resistance in the four first layers calculated from both the heating period and the recovery period. Photo: Petri Hakala, GTK.

tivity is 3.82 W/(m·K) and the borehole thermal resistance is 0.078 (m·K)/W. The analytical fluid temperature profile calculated with parameter values determined separately for each layer, like the preceding values representing layer 1, is the solid black line in Figures 18 and 19. When using the infinite line source method combined with the superposition technique (heat rate during injection Q = const. and during recovery Q = 0), thermal conductivity is calculated from recovery data at first (blue solid line), while the thermal resistance is zero. Then, adjusting the preceding calculated temperature data (blue solid line) for the measured data in the heating period (purple solid line) and minimizing the error between them, the borehole thermal resistance is also optimized utilizing the superposition technique (red solid line). As one

can see, there is some difference between values calculated with these two time periods. Finding the optimal fitting period in heating and recovery phases is important, since it has large effect on the final result. The first 10 hours of heat injection data were disregarded due to thermal capacity effects. The results demonstrate that thermal conductivity obtains its lowest values in the second and sixth layers.

Figure 20 combines the results presented above in Figures 18 and 19. Layered thermal conductivity was determined from the recovery period as well as the heating period. Figure 20 shows that parameters solved using the infinite line source method combined with variable heat rates, i.e. the superposition technique applied to the recovery data (blue solid line), are smaller than the
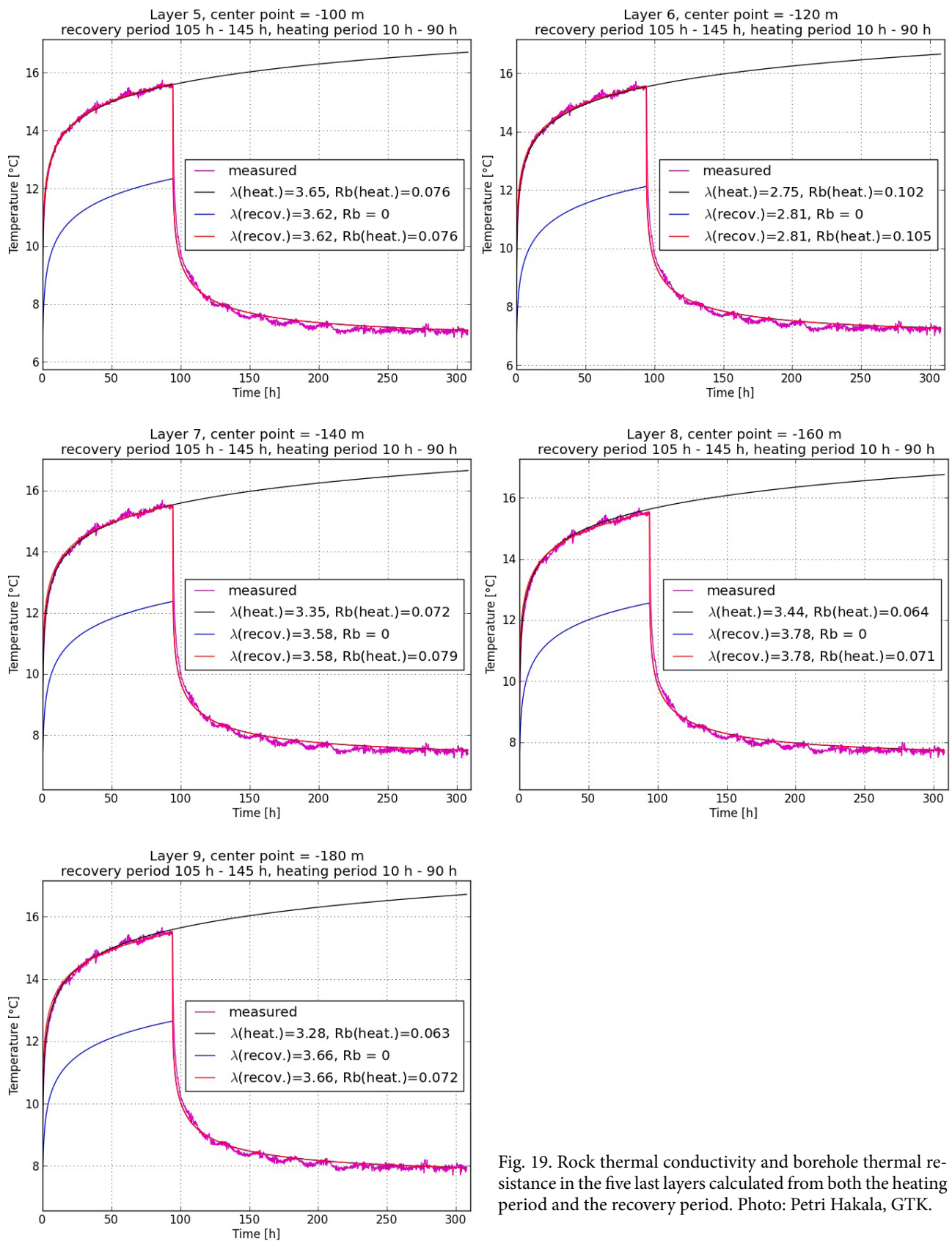
Fig. 19. Rock thermal conductivity and borehole thermal resistance in the five last layers calculated from both the heating period and the recovery period. Photo: Petri Hakala, GTK.
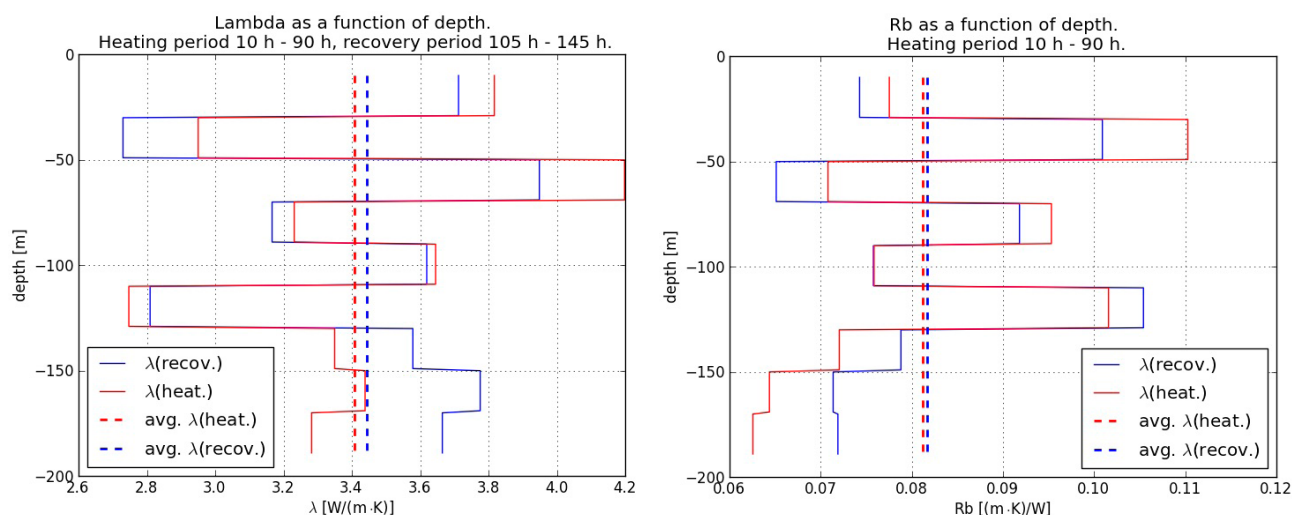
Fig. 20. The layered thermal conductivities achieved from the recovery and heat injection data (on the left), and the layered thermal resistance of the borehole (on the right). The layered thermal conductivity calculated from the recovery period is represented by the blue solid line and the layered thermal conductivity calculated from the heating period by the red solid line. The dashed lines correspondingly indicate the averaged value of all nine layers obtained using constant heat power and a variable heat rate. Photo: Petri Hakala, GTK.

infinite line source results solved using constant heat power applied to the heat injection data (red solid line) on the five first layers, but gives a larger value in the final sections. These acquired thermal conductivities in different sections of the BHE were then used as an input parameter when optimizing the layered borehole thermal resistance from the heating period. The red dashed line represents the average value of all nine layers obtained using constant heat power (conductivity calculated from the heat injection period), while the blue dashed line represents the respective average value obtained using a variable heat rate (conductivity calculated from the recovery period).

According to the SEM analysis, the third layer, which is defined by the depth interval 50–70 m,

has the lowest quartz content, referring to a lower thermal conductivity. However, as can be seen in Figure 20, the third layer has the highest thermal conductivity of all sections. This indicates that the soya powder samples may not have been taken precisely from the particular depth interval, i.e. that the sampling depth was not exact. In contrast, the second layer, representing the depth interval 30–50 m, correlates well with SEM analysis. The soya powder samples were collected around the depth of 50 m. Comparing the quartz content and the thermal conductivity deeper in the borehole, in layers 8 (150–170 m) and 9 (170–190 m), the correlation is clear. The thermal conductivity of the bedrock increases as a function of the quartz content.

6.6 Theoretical estimates of the borehole thermal resistance

Since the measured average thermal resistance of the BHE was approximately 0.08 (m·K)/W, as was pointed out in chapters 6.4 and 6.5, it can now be compared with the theoretical borehole thermal resistances presented in this chapter.

There were no spacers between the U pipes, meaning that the pipe positions in the borehole were unknown. It is well known and experimentally proven that borehole thermal resistance depends on the distance between pipes in the borehole. Thermal coupling between pipe shanks should be minimized, and this occurs when the pipes are close to the borehole wall, as seen in Fig-

ure 21 on the right, i.e. the temperature difference between the borehole wall and the heat carrier fluid is as small as possible.

The polyethylene pipe has an outer and inner diameter of 40 mm and 35.2 mm, respectively, and because the thermal conductivity of pipe material is approximately 0.42 W/(m·K), the thermal resistance due to the pipe material is R_p = 0.048 (m·K)/W according to equation (12). The flow rate during TRT measurement was 48.75 liters per minute, i.e. the average fluid velocity in the pipe was 0.84 m/s. Since the density of the heat carrier fluid is 960 kg/m³ and dynamic

viscosity 0.00134 kg/(m·s) (manufacturer's product sheet, Altia Plc), the Reynolds number for fluid flow is approximately 21055, i.e. the fluid flow is in a fully developed turbulent state. According to equation (7), the dimensionless Nusselt number for turbulent flow calculated using thermal conductivity and specific heat capacity values of 0.39 W/(m·K) and 3640 J/(kg·K) is 194.3. Therefore, the convective heat transfer coefficient for turbulent flow in this case is approximately 2153 W/(m²·K) and the thermal resistance due to fluid flow calculated using equation (5) is then R_f = 0.0042 (m·K)/W, i.e. almost 12 times smaller than that of pipe material. Theoretical equations for thermal resistance of the borehole filling material presented in Chapter 3.2 do not take into account the groundwater convective effect on the heat transfer efficiency. This is the main reason why the estimated borehole thermal resistance is usually larger than that calculated from TRT or DTRT data using the infinite line or cylinder source method.

The following, Table 2 presents the theoretical resistances of the BHE calculated with three different equations representing the borehole filling material, i.e. Hellström, Bennet, and Sharqawy (see Chapter 3.2). These equations are valid in groundwater-filled boreholes only when the water is considered as a solid material. The individual resistances of the pipe material and fluid flow were also taken into account when calculating the borehole thermal resistance. Results were obtained with two different pipe positions: In the first configuration, the pipes were close to each other near the borehole center, and in the second configuration, the pipes were in direct contact with the borehole wall according to Figure 21. The groundwater thermal conductivity was assumed to be 0.6 W/(m·K) and the rock thermal conductivity was set to a value 3.5 W/(m·K).

The measured borehole thermal resistance was 0.08 (m·K)/W, i.e. it appears that Hellström's equation overestimates the true thermal resistance. The minimum theoretical value is obtained when the pipes are apart from each other. In this case, Hellström's equation gave a value 0.112 (m·K)/W. In contrast, resistances calculated with the Bennet and Sharqawy equations matched bet-
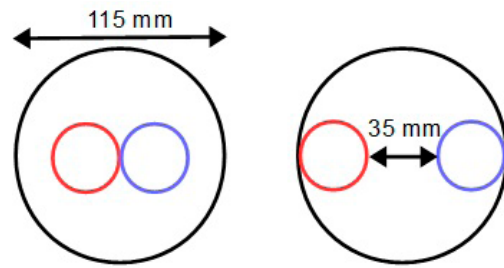

Fig. 21. A cross-section of the borehole and the location of the pipes. Photo: Petri Hakala, GTK.

Table 2. Borehole theoretical resistances [(m·K)/W] calculated with three different equations and two pipe positions: the pipes close to each other and apart from each other, close to the borehole wall (ds = center-to-center distance).

Equation	ds = 50 mm	ds = 75 mm
Hellström	0.182	0.112
Bennet et al.	0.158	0.083
Sharqawy et al.	0.154	0.068

ter with the measured value. During the DTRT measurement, the pipes were probably close to the borehole wall, and the center-to-center distance between the pipes did not therefore differ much from the value of 75 mm. In other words, the Bennet method predicts the resistance in this specific case somewhat more accurately than the Hellström or Sharqawy equations.

Fluid temperature values obtained from the conventional or distributed thermal response test and analysis with the infinite line source method gave the best approximation of the true borehole thermal resistance. However, if experimental measurements are not possible, the borehole thermal resistance can be evaluated with the theoretical approach presented in Chapter 3.3, which also indicates how the results presented in Table 2 were calculated, i.e. as a sum of individual thermal resistances of the borehole filling, pipe material, and heat carrier fluid ($R_b = R_g + R_p / 2 + R_f/2$). The borehole thermal resistance value obtained with theoretical equations might, however, overestimate the true value, since natural convection is not taken into account. The temperature difference between the borehole wall and heat carrier fluid enhances the natural convection of the groundwater, and thus reduces the borehole thermal resistance.

6.7 Uncertainty in parameter estimation

Temperature measurements via DTS and analytical interpretation are both possible error sources when estimating the bedrock thermal conductivity and borehole thermal resistance. A high spatial temperature resolution can be achieved if the operating temperature of the DTS instrument is nearly constant during the whole measuring period and the DC voltage of the power supply remains stable. In practice, this was not completely attained, because the DTS device was subjected to air temperature variations. This technical aspect of measurement has an influence on the interpretation of the thermal parameters. The effects of a varying operating temperature on DTS accuracy could be tested, for example, by placing an optical fiber in an ice bath (known temperature) and changing the ambient temperature.

During DTRT measurements at the Nupurinkartano study site, the DTS instrument was exposed to the varying outside temperature, since it was placed inside a TRT rig (light insulation). Temperature drift due to internal temperature changes is not extensively discussed in the literature. However, Tyler et al. (2009) have noted changes of up to 1 to 2 $^{\circ}$C when subjecting the DTS device to temperature variation during multi-day measurements. DTRT measurement at Nupurinkartano took almost 13 days. Temperature variations may have induced error in the heat power calculation, since it was directly calculated using the measured temperature difference between ascending and descending pipe shanks in each section. This means that if there is uncertainty in temperature measurement, it will directly affect the heat power

calculation and furthermore the interpretation of data.

An analytical infinite line source equation was fitted to the fluid measured average temperature by optimizing the bedrock thermal conductivity and borehole thermal resistance in each layer, minimizing the error between the measured and calculated average fluid temperature. Determining the optimal fitting period in heating and recovery phases is important, since it has large effect on the final result, especially if the chosen period is too short. The first 10 hours of heat injection data were disregarded due to thermal capacity effects. Moreover, the diurnal temperature drift needs to be taken into account, because it influences the slope determination and thus the thermal conductivity calculation. The heterogeneity in the estimation of the layered thermal conductivity may be attributed to both the measurement technology and interpretation aspects.

Layered thermal conductivities acquired from heating and recovery data were used as an input parameter when optimizing the layered borehole thermal resistance from heat injection data. Thus, possible errors related, for example, to temperature measurements, data quality, the temperature drift, and heat power fluctuations accumulate when estimating borehole thermal resistance. In addition, the heterogeneity of borehole thermal resistance could be due to convective heat transfer in the groundwater, which was not considered in this study, or possibly the lateral deviation in the U-pipe along the borehole depth.

7 SUMMARY AND CONCLUSIONS

In this study, the distributed thermal response test was evaluated in the Nupurinkartano test area. The purpose was to assess the DTRT method in its entirety, from measurements to interpretation and the utilization of the results. Furthermore, the thermal conductivity of the bedrock and thermal resistance of the borehole determined via conventional and distributed thermal response tests were compared. Nupurinkartano was selected as a test area because GTK has *in situ* knowledge of the geological conditions and the composition and the structure of the bedrock at the site. In 2008, GTK

conducted geophysical measurements in order to dimension and model the GSHP system. Borehole geophysical measurements and scanning of the borehole were also carried out at the request of the customer at the time.

The borehole installation studied was groundwater-filled, 115 mm in diameter and had an active depth of 197.2 meters. Optical fiber cables were placed inside both shanks of the U-pipe to measure the temperature of the heat carrier fluid along the total length of the BHE. During the conventional thermal response test, the average fluid

temperature is usually only logged from the inlet and outlet section of the BHE, differing somewhat from the true average fluid temperature measured by optical fiber cables. The ground averages, i.e. effective thermal parameters, were evaluated from the heating period 10–90 hours. The resulting average thermal conductivity varied between 3.47–3.53 W/(m·K) and the average thermal resistance between 0.081–0.083 K/(W/m), depending on whether the variable heat rate effects were taken into account. A comparable fit for the same heating period and the same interpretation techniques was also carried out for the true average temperature measured using optical fiber cables consisting of all measured temperatures at each depth. The corresponding results for the effective (average) thermal conductivity varied between 3.46–3.51 W/(m·K) and for the average thermal resistance 0.075–0.077 K/(W/m). As a conclusion, the borehole thermal resistance calculated with the arithmetic mean temperature from the ground surface slightly overestimates the true value. Thus, the resistance is slightly higher if the average fluid temperature is calculated as the arithmetic mean of the inlet and the outlet section instead of the true average temperature. However, there were no notable differences in the thermal conductivity.

The DTRT carried out in this work consisted of four different phases and lasted almost 310 hours in total. In the first phase, the undisturbed ground temperature was measured without circulating heat carrier fluid. This was followed by the second phase, in which a pre-circulation of the fluid without heating was carried out for one hour. Subsequently, in the third phase, a constant heat power was injected for 94 hours. Finally, in the fourth phase, borehole recovery was observed by measuring the temperature with no heating or fluid circulation during 216 hours.

To determine the layered thermal conductivity and layered thermal resistance, the borehole was divided into nine sections, each of 20 meters in length. However, first and last ten meters of the BHE length were disregarded. Thus, the influence of the ambient air and disturbances of fiber splicing at the bottom of the borehole were eliminated. By applying the line source method to each layer and fitting the calculated fluid temperatures to the measured ones, the thermal conductivity of the bedrock was optimized and solved in different sections of the BHE. The true average temperature of the heat carrier fluid was calculated with six temperature values, i.e. three in each pipe within each layer at different times. In this way, the layered thermal conductivity was assessed during both heating and recovery periods. However, evaluation of the recovery period is usually more recommendable. It is notable that the data logged in the recovery phase allow the determination of layered thermal conductivity but not thermal resistance, because the injected heat power is almost zero and there is no temperature difference between the borehole wall and heat carrier fluid. Finally, as a result, the thermal conductivity varied between 2.8–4.2 W/(m·K) in different sections of the borehole, depending on whether the variable heat rate effects were taken into account. Layered thermal conductivities acquired from heating and recovery data were then used as input parameters when optimizing the borehole thermal resistance from heat injection data defined from the heating period of 10–90 hours. Finally, the layered thermal resistance of the borehole was determined, and it was found to vary from 0.06–0.11 K/(W/m) between different sections of the BHE.

According to the SEM analysis, the third layer, which was defined as the depth interval 50–70 m, had the lowest quartz content, suggesting a lower thermal conductivity. However, our DTRT interpretation results gave the highest thermal conductivity in this third layer. This indicates that the soya powder samples may not have been taken precisely from a particular depth, i.e. that the sampling depth was not exact. In contrast, the second layer, which was defined as the depth interval 30–50 m, correlated well with SEM analysis. The soya powder samples in this layer were collected around the depth of 50 m. Comparing the quartz content and the thermal conductivity deeper in the borehole, in layer 8 (150–170 m) and layer 9 (170–190 m), the correlation was clear. The thermal conductivity increased as a function of the quartz content.

Geologically, the study area was considered as homogeneous granite. The borehole geophysical investigations conducted earlier indicated that the bedrock is homogeneous and solid, with no notable changes in rock type being detected. The results from the SEM analysis indicated good thermal conductivity because of the reasonably high quartz content. Thus, the differences in the estimation of the layered thermal conductivity may be attributed to both the measurement technology and interpretation aspects. The DTS device was subjected to air temperature variations, and the

temperature measured with the optical fiber cables was therefore affected by diurnal temperature variations. Uncertainty in temperature measurement affects the heat power calculation and furthermore the estimation of thermal conductivity. Moreover, the selection of the appropriate fitting period and layer sectioning may influence the heterogeneity in thermal conductivity.

Heterogeneity in the estimation of the borehole thermal resistance can be accumulated from the acquired layered thermal conductivity, which was used as an input parameter when optimizing the layered borehole thermal resistance. Thus, possible errors related, for instance, to temperature measurements, temperature drift, data quality, and heat rate fluctuations accumulate when estimating borehole thermal resistance, producing bias. In addition, heterogeneity in the borehole thermal resistance can be due to convective heat transfer in the groundwater, which was not considered in this study, or possibly to lateral deviation of the U-pipe along the borehole depth. In this study, the infinite line source method combined with the superposition technique, i.e. utilizing variable heat rates applied to the recovery data, gave a lower thermal conductivity and thermal resistance in the upper section of the borehole, but larger values in the final section.

The DTRT method clearly provides a more detailed overview along the borehole, which is significant in a heterogeneous and anisotropic environment. With DTRT it is possible to detect fissures and cracks where groundwater movements occur, which is not the case with the conventional method. On the other hand, the DTRT procedure takes a longer time to perform than the conventional TRT procedure due to the recovery phase. Thus, simply using optical fiber cables to measure the true average temperature also enables a more accurate estimation of the effective thermal parameters from the heating period. Furthermore, the layered thermal conductivity and borehole thermal resistance should be possible to utilize in software for designing borehole field systems, which is not the case with current commercial programs.

In future work, our goal is to improve the interpretation methods related to TRT and DTRT. Beginning with improving the data quality and management, detecting the source of errors and paying attention to the determination of the optimal fitting period, the layer sectioning and also the fluctuations in the heat power, we believe it will be possible to obtain more reliable and accurate results.

REFERENCES

Acuña, J. 2013. Distributed thermal response tests – New insights on U-pipe and Coaxial heat exchangers in groundwater-filled boreholes. Stockholm: Royal Institute of Technology (KTH). 141 p. (dissertation)

Acuña, J., Mogensen, P. & Palm, B. 2008. Distributed thermal response test on a U-pipe borehole heat exchanger. The 8th IIR Gustav Lorentzen Conference, Copenhagen. 8 p.

Al-Khoury, R. 2012. Computational Modeling of Shallow Geothermal Systems. London, UK: CRC Press Taylor & Francis group. (eBook)

Altia Plc. Teollisuusetanolit [Electronic resource]. Available at: www.altiacorporation.fi/fi/Tuotanto/Tekniset+etanolit/Tuotteet/ (in Finnish)

Bennet, J., Claesson, J. & G. Hellström, G. 1987. Multipole Method to Compute the Conductive Heat Flows to and between pipes in a composite cylinder. Dep. of Building Tecnology and Mathematical Physics, Lund institute of Technology, Notes on Heat Transfer. 41 p.

Eklöf, C. & Gehlin, S. 1996. TED – a mobile equipment for thermal response test. MSc -thesis, Luleå university of technology. 62 p.

Fujii, H., Okubo, H. & Itoi, R. 2006. Thermal Response Tests Using Optical Fiber Thermometers. GRC Transactions 30, 545−551.

Gustafsson, A.-M. & Westerlund, L. 2010. Multi-injection rate thermal response test in groundwater filled borehole heat exchanger. Renewable Energy 35, 1061−1070.

Hellström, G. 1991. Ground Heat Storage; Thermal Analysis of Duct Storage Systems. Department of Mathematical Physics, University of Lund, Sweden. 310 p. (dissertation)

Incropera, F. P & Dewitt, D. P. 2002. Fundamentals of Heat and Mass Transfer. John Wiley & Sons. 5th edition. 1008 p.

Kielosto, S., Sten, C-G. & Juntunen, R. 2002. Nuuksion kartta-alueen maaperä, maaperäkartan selitys 1:20 000 – Explanation to Maps of Quaternary deposits, Sheet 2041 10. Geological Survey of Finland. 13 p. (in Finnish)

Lamarche, L., Kajl, S. & Beauchamp, B. 2010. A review of methods to evaluate borehole thermal resistances in geothermal heat-pump systems. Geothermics 39, 187−200.

Leppäharju, N., Engström, J., Kallio, J., Nordbäck, N. & Tiensuu, K. 2008. Nupurinkartanon geoenergiatutkimukset. Tilaustutkimusraportti, Geological Survey of Finland. 13 p. (in Finnish)

Marcotte, D. & Pasquier, P. 2008. On the estimation of thermal resistance in borehole thermal conductivity test. Renewable Energy 33, 2407−2414.

Mogensen, P. 1983. Fluid to Duct Wall Heat Transfer in Duct System Heat Storages. Proceedings of the International Conference on Subsurface Heat Storage in Theory and

Practice. Stockholm, Sweden. 7 p.

Monzó, P. 2011. Comparison of different Line Source Model approaches for analysis of Thermal Response Test in a U-pipe Borehole Heat Exchanger. MSc –thesis, KTH School of Industrial Engineering and Management, Stockholm, Sweden. 97 p.

Philippe, M., Bernier, M. & Marchio, D. 2009. Validity ranges of three analytical solutions to heat transfer in the vicinity of single boreholes. Geothermics 38, 407–413.

Peltoniemi, S. 1996. Relationships between thermal and other petrophysical properties of rocks in Finland. MSc -thesis. Espoo: Teknillinen korkeakoulu. 100 p.

Raymond, J., Therrien, R., Gosselin, L. & Lefebvre, R. 2011. A Review of Thermal Response Test Analysis Using Pumping Test Concepts. Groundwater 49 (6), 932–945.

Tyler, S. W., Selker, J. S., Hausner, M. B., Hatch, C. E., Torgersen, T., Thodal, C. E. & Schladow, S. G. 2009. Environmental Temperature Sensing using Raman Spectra DTS Fiber-Optic Methods. Water Resources Research, vol. 45. 11 p.

Selker, J. S., Thévenaz, L., Huwald, H., Mallet, A., Luxemburg, W., van de Giesen, N., Stejskal, M., Zeman, J., Westhoff, M. & Parlange, M. B. 2006a. Distributed fiber-optic temperature sensing for hydrologic systems. Water Resources Research, vol. 42. 8 p.

Selker, J., van de Giesen, N., Westhoff, M., Luxemburg, W. & Parlange, M. B. 2006b. Fiber optics opens window on stream dynamics. Geophysical Research Letters, vol. 33. 4 p.

Sharqawy, M., Mokheimer, E. M. & Badr, H. M. 2009. Effective pipe-to-borehole thermal resistance for vertical ground heat exchangers. Geothermics 38, 271–277.

Yang, H., Cui, P. & Fang, Z. 2010. Vertical-borehole ground-coupled heat pumps: A review of models and systems. Applied Energy 87, 16–27.

The Thermal Response Test (TRT) is a method for determining the thermal resistance of a Borehole Heat Exchanger (BHE) and the thermal conductivity of the ground surrounding it. These are important parameters that are used in designing large BHE fields. During a TRT, the temperature of the heat carrier fluid is recorded at the inlet and outlet of the heat collector pipe of a BHE. The recorded temperatures are then used to solve the average borehole thermal resistance and ground thermal conductivity.

The Distributed Thermal Response Test (DTRT) is a new way of carrying out the TRT. Instead of only recording the heat carrier fluid temperature at the inlet and outlet, it is recorded along the entire length of the heat collector pipe. This additional information enables the solution of the borehole thermal resistance and ground thermal conductivity as a function of depth.

In this report, an evaluation of the DTRT method in a Finnish setting is presented. The theory behind the DTRT is first summarized, and the DTRT measurements carried out in a BHE located in Nupurinkartano, Southern Finland, are then described. Finally, the interpretation of the DTRT measurements is presented. Detailed information on the vertical distribution of ground thermal conductivity is obviously important in heterogeneous or fractured bedrock conditions.

All GTK's publications online at hakku.gtk.fi